AD_____

Award Number: DAMD17-03-1-0087

TITLE: Erbium: YAG Laser Incision of Urethral Strictures for Treatment of Urinary Incontinence after Prostate Cancer Surgery

PRINCIPAL INVESTIGATOR: Nathaniel Fried, Ph.D.

CONTRACTING ORGANIZATION: Johns Hopkins University
School of Medicine
Baltimore, Maryland 21205

REPORT DATE: February 2004

TYPE OF REPORT: Annual

PREPARED FOR: U.S. Army Medical Research and Materiel Command
Fort Detrick, Maryland 21702-5012

REPORT DOCUMENTATION PAGE

Form Approved
OMB No. 074-0188

1. AGENCY USE ONLY (Leave blank)	2. REPORT DATE	3. REPORT TYPE AND DATES COVERED
	February 2004	Annual (1 Feb 03-31 Jan 04)

4. TITLE AND SUBTITLE
Erbium: YAG Laser Incision of Urethral Strictures for Treatment of Urinary Incontinence after Prostate Cancer Surgery

5. FUNDING NUMBERS
DAMD17-03-1-0087

6. AUTHOR(S)
Nathaniel Fried, Ph.D.

7. PERFORMING ORGANIZATION NAME(S) AND ADDRESS(ES)
Johns Hopkins University School of Medicine
Baltimore, Maryland 21205

E-Mail: nfried@jhmi.edu

8. PERFORMING ORGANIZATION REPORT NUMBER

9. SPONSORING / MONITORING AGENCY NAME(S) AND ADDRESS(ES)
U.S. Army Medical Research and Materiel Command
Fort Detrick, Maryland 21702-5012

10. SPONSORING / MONITORING AGENCY REPORT NUMBER

11. SUPPLEMENTARY NOTES
Original contains color plates. All DTIC reproductions will be in black and white.

12a. DISTRIBUTION / AVAILABILITY STATEMENT
Approved for Public Release; Distribution Unlimited

12b. DISTRIBUTION CODE

13. ABSTRACT (Maximum 200 Words)
Urethral and bladder neck strictures occur in 5-20 % of all prostate cancer surgeries, resulting in urinary incontinence. Conventional treatments for stricture (including balloon dilation, cold knife incision, electrocautery, and Holmium laser incision) have widely variable success rates with sub-optimal long-term results. The failure of these conventional stricture treatments is presumably due to mechanical and/or thermal damage to the urethral wall during the procedure. The purpose of this research project is to test a new laser, the Erbium:YAG laser, which is capable of precisely incising the urethral stricture with minimal peripheral damage to adjacent healthy tissue. We hypothesize that the minimal side-effects caused during Erbium laser incision should translate into limited scarring and improved procedural success rates. The first year of this project was devoted to optimization of the laser and optical fiber delivery system for rapid and precise cutting of urethral tissue. We have successfully accomplished these tasks, and published our findings in the form of four manuscripts and two abstracts.

14. SUBJECT TERMS
No subject terms provided.

15. NUMBER OF PAGES
50

16. PRICE CODE

17. SECURITY CLASSIFICATION OF REPORT	18. SECURITY CLASSIFICATION OF THIS PAGE	19. SECURITY CLASSIFICATION OF ABSTRACT	20. LIMITATION OF ABSTRACT
Unclassified	Unclassified	Unclassified	Unlimited

TABLE OF CONTENTS

Cover.....1

SF 298.....2

Introduction.....4

Body.....4

Key Research Accomplishments.....15

Reportable Outcomes.....16

Conclusions.....17

References.....18

Appendices.....19

INTRODUCTION

Urethral and bladder neck strictures occur in 5-20 % of all prostate cancer surgeries, resulting in urinary incontinence [1,2]. Conventional treatments for stricture (including balloon dilation, cold knife incision, electrocautery, and Holmium laser incision) have widely variable success rates with sub-optimal long-term results [3-6]. The failure of these conventional stricture treatments is presumably due to mechanical and/or thermal damage to the urethral wall during the procedure. The purpose of this research project is to test a new laser, the Erbium:YAG laser, which is capable of precisely incising the urethral stricture with minimal peripheral damage to adjacent healthy tissue [7,8]. We hypothesize that the minimal side-effects caused during Erbium laser incision should translate into limited scarring and improved procedural success rates. The first year of this project was devoted to optimization of the laser [9] and optical fiber delivery system [10] for rapid and precise cutting of urethral tissue. We have successfully accomplished these tasks, and published our findings in the form of four manuscripts and two abstracts.

BODY

Below is a list of the tasks from the approved "Statement of Work" for Year 1.

YEAR 1

Task #1. Modification of Erbium:YAG laser system (Months 1-6)

a. Modify electronics in laser power supply to produce shorter laser pulses, more uniform temporal beam profile, and higher pulse repetition rates.

b. Optimize laser ablation parameters (laser energy, pulse duration, repetition rate, and irradiation time) using in vitro tissue samples.

Task #2. Determination of optimal optical fiber delivery system (Months 7-12)

a. Test fiber optic damage thresholds with chemical and microscopic analysis of fiber tips after laser ablation with fiber in contact with tissue.

b. Design side-firing laser fibers w/ varying delivery angles for incision of urethral wall.

c. Build hybrid fibers combining flexible germanium oxide trunk fiber with durable sapphire probe tip to prevent fiber damage.

Table 1. Status of assigned tasks in the "Statement of Work"

Task	Status	Description
1.a	Completed	P. 5
1.b	Competed	Pp. 6-8
2.a	Completed	Pp. 9-10
2.b	Not Completed - Unnecessary	Pp. 11
2.c	Completed	Pp. 11-14

Task 1.a. Modification of Erbium Laser

Problem: Our original Erbium:YAG laser system was limited by a fixed laser pulse length of approximately 250 μs and a low pulse repetition rate of less than 5 Hz. These laser parameters are sub-optimal for rapid and precise cutting of the urethra and bladder neck. The long laser pulse duration results in more peripheral thermal damage to adjacent tissue than is necessary and the low pulse repetition rate prevents rapid tissue removal, which is required for clinical use.

Solution: We replaced our original high-voltage laser power supply with a variable pulse power supply (Model 8800V, Analog Modules, Orlando, FL). This power supply allowed us to operate the Erbium:YAG laser system with pulse lengths ranging from 1-500 μs and with pulse repetition rates of 1-50 Hz. Figure 1abc shows the shorter pulse lengths achieved with the variable power supply, while Figure 1d shows the long-pulse profile of our original laser system.

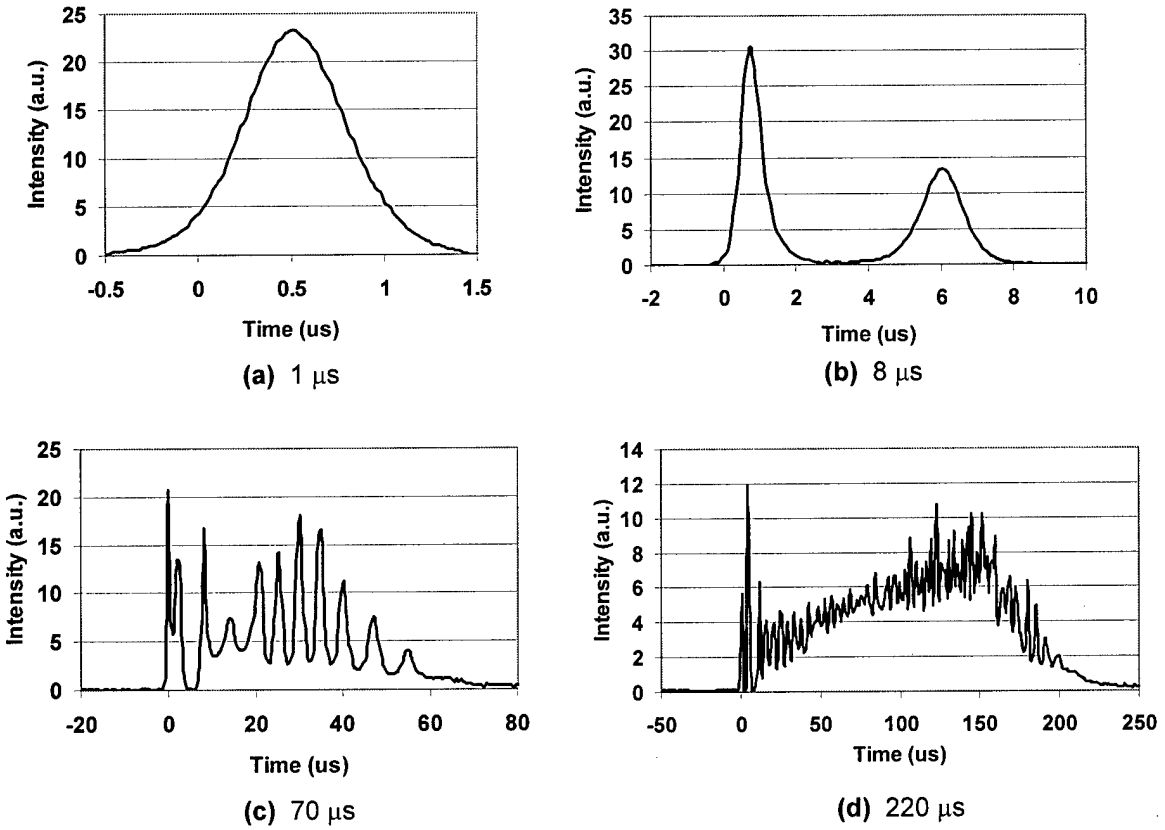

Figure 1. Temporal pulse profiles for Er:YAG laser operated with pulse lengths of 1, 8, 70, and 220 μs.

Task 1.b. Optimize Laser Ablation Parameters with In Vitro Tissue Samples
Problem: The optimal laser parameters (laser energy, pulse length, repetition rate, and irradiation time) for precision cutting of urethral tissue have never been studied.
Solution: Studies were conducted to determine the laser parameters which provided the most rapid and efficient cutting of urethral tissue, while also minimizing peripheral thermal damage to surrounding healthy tissue.

Tissue Studies

Fresh prostatic urethral tissue samples were obtained from male dogs (25-30 kg) after sacrifice for unrelated experiments at the Johns Hopkins Medical School. The posterior urethra was dissected from the prostate, spatulated, sectioned into 1 x 1 cm samples, stored in saline, and refrigerated. For the ablation measurements, tissue samples were sandwiched between microscope and plexiglass slides to a fixed thickness (350 $\pm$ 50 μm), and the optical fiber tip positioned in contact with the sample through 2-mm-diameter holes drilled in the front plexiglass holder. The tissue samples were kept hydrated with saline using a syringe during the ablation experiments. The samples were placed in front of a pyroelectric detector, and the number of pulses required to perforate each sample was measured.

Ablation Results

The Er:YAG ablation rates are shown in Figure 2 for the ex vivo tissue experiments. Perforation of the tissue samples was achieved at laser fluences of 3-5 J/cm^2 and pulse energies of 1.5 - 2.5 mJ, without advancing the fiber into the tissue. There was an almost two-fold increase in the ablation rate for a given fluence when reducing the laser pulse duration from 220 μs to 70 μs. The 220-μs line shows an ablation rate of 4 μm per J/cm^2, while the 70-μs line shows an ablation rate of 7 μm per J/cm^2. Reducing the pulse length to 8 μs produced a minor increase in the ablation rate, but at the expense of much lower laser energy output and peripheral mechanical tissue damage.

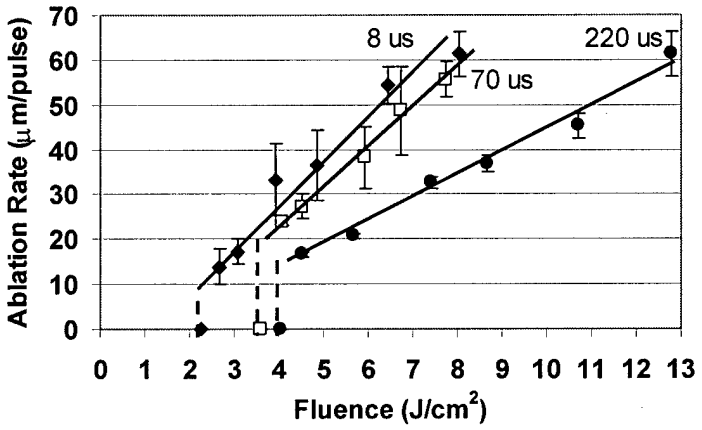

Figure 2. Er:YAG ablation rates using laser pulse lengths of 8, 70, 220 μs, and plotted as a function of laser fluence. Bars signify mean values $\pm$ S.D. (n=6). Note that the perforation threshold decreases as the laser pulse is decreased, and ablation is also more efficient.

Figure 2 demonstrates that we can predict exactly how much tissue is removed per laser pulse as a function of the laser energy and pulse length, and therefore we can precisely control the incision depth during Erbium laser treatment of strictures. Figure 2 also demonstrates that by shortening the laser pulse length from 220 μs to 70 μs, we can almost double the rate at which tissue is removed, making the Erbium laser more efficient.

Thermal Damage Measurements

Histological measurements of thermal damage were conducted as a function of laser pulse duration. The results for the ex vivo tissue studies are shown in Figure 3. When the Er:YAG laser was operated in its normal long pulse mode (220 μs pulse length), a thermal damage zone of 30-60 μm was observed. Shortening the laser pulse to 70 μs resulted in a reduction of the thermal damage to 15-30 μm. The shortest laser pulse, measuring 8 μs, further reduced the thermal damage zone to 10-20 μm, but also resulted in a rougher cut, due to mechanical tissue-tearing effects. ***Figure 3 shows that by shortening the laser pulse length from 220 μs to 70 μs, we also decrease the amount of undesirable peripheral thermal damage by a factor of 2.***

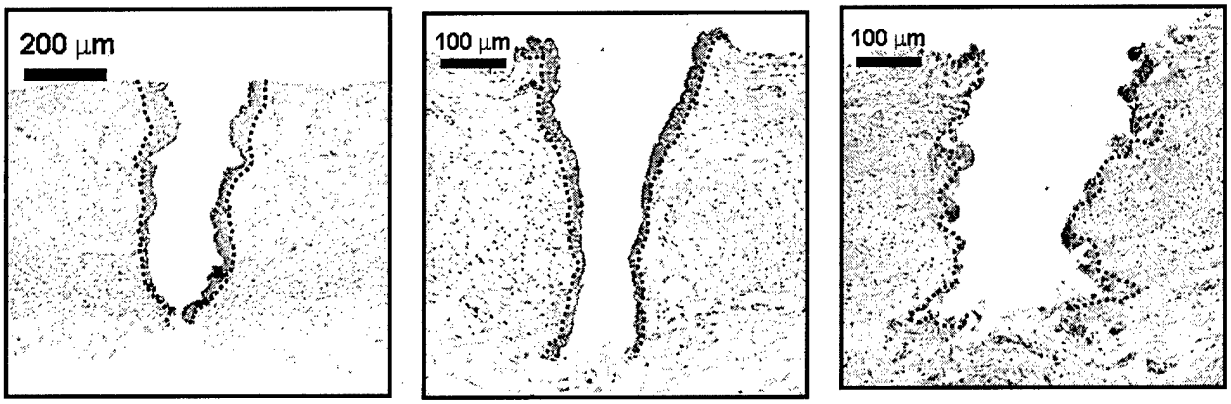

(a) 220 μs; Damage: 30-60 μm **(b)** 70 μs; Damage: 15-30 μm **(c)** 8 μs; Damage: 10-20 μm

Figure 3. Photomicrographs showing H&E stained histologic cross-sections of ureteral tissues ablated with the Er:YAG laser, ex vivo. The thermal damage zone decreases as the laser pulse duration is decreased. Rough, jagged borders of the ablation crater produced by 8 μs laser pulses may be due to mechanical tissue-tearing caused during ablation.

An ex vivo study was also performed to determine whether the thermal damage zone would increase with laser operation at higher pulse repetition rates, due to residual heat accumulation in the tissue with deposition of successive laser pulses. The pulse duration, energy per pulse, and total number of pulses were all kept constant at 70 μs, 10 mJ, and 20 pulses (total energy = 200 mJ), respectively, while the pulse repetition rate was varied from 10-30 Hz. The thermal damage zone increased as the laser pulse repetition rate increased, and a large increase in thermal damage was observed when the pulse repetition rate was increased from 20 to 30 Hz (Figure 4).

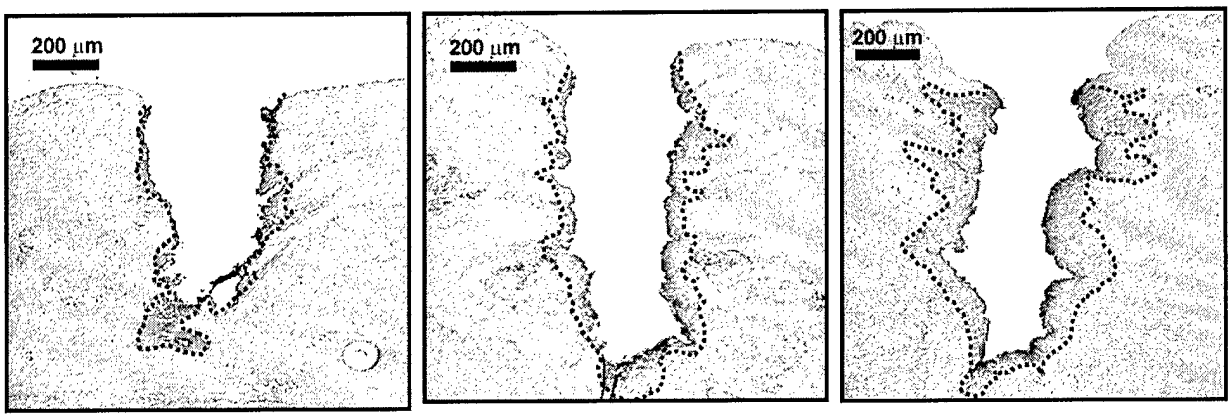

(a) 10 Hz; Damage: 20-40 μm **(b)** 20 Hz; Damage: 30-60 μm **(c)** 30 Hz; Damage: 60-120 μm

Figure 4. Photomicrographs showing H&E stained histologic cross-sections of urethral tissues ablated with the Er:YAG laser, ex vivo, with varying laser pulse repetition rates of 10–30 Hz. Energy was kept fixed at 10 mJ per pulse with a total of 20 pulses (200 mJ) delivered to the tissue. Note that there is a large increase in the thermal damage zone from 20 – 30 Hz, due to residual heat accumulation in the tissue during ablation. The dotted lines demarcate the border of the thermal damage zone.

Figure 4 shows that if the Erbium:YAG laser is operated at a pulse repetition rate higher than approximately 20 pulses per second, then the peripheral thermal damage to adjacent healthy tissue will increase and reach unacceptable levels, capable of causing increased scarring and increased probability of stricture recurrence.

The Er:YAG laser, operating at a pulse duration of ~ 70 μs, a fluence of 4 J/cm^2, and a repetition rate of 20 Hz, is capable of rapidly incising urethral tissues with minimal thermal and mechanical side-effects. The Er:YAG laser is more efficient than the Ho:YAG laser for cutting ureteral and urethral tissues, with perforation thresholds measuring 2 J/cm^2 versus 34 J/cm^2, respectively. The Er:YAG laser is also more precise than the Ho:YAG laser, with peripheral thermal damage zones measuring 10-20 μm versus 300 μm, respectively.

Task 2.a. Test Damage Thresholds of Optical Fibers

Problem: Erbium:YAG laser energy (wavelength = 2.94 μm) cannot be delivered through conventional silica optical fibers because glass does not transmit light at wavelengths beyond approximately 2.5 μm. Specialty mid-infrared optical fibers are needed to transmit the Erbium:YAG laser energy. Although there are several types of optical fibers and waveguides available for delivery of mid-infrared laser radiation, including chalcogenide, zirconium fluoride, sapphire, germanium oxide, and hollow silica waveguides, all of these delivery systems have major limitations [11,12]. The chalcogenide fibers cannot handle high power, they are toxic, and they break easily. The zirconium fluoride fibers are also brittle, hygroscopic, and toxic in tissue. The sapphire fibers suffer from mechanical stress and breakage during tight bending conditions. The germanium oxide fibers have a low melting temperature preventing their use in contact mode at high powers. The hollow silica waveguides are not biocompatible and have limited bending ability with high transmission losses during tight bending. Thus, the ideal mid-infrared optical fiber that combines high-power delivery, flexibility, chemical and mechanical durability, and biocompatibility, has yet to be developed.

Solution: The germanium oxide optical fiber represents the most promising type of mid-infrared fiber for use in treating strictures because it is capable of delivering high laser power and it is also the most flexible of the mid-infrared fibers, making it suitable for use with flexible endoscopes in urology [13]. The goal of this study was to determine the limitations of the germanium fiber, and identify areas at which it can be improved for use as an optical fiber delivery system for the treatment of urethral and bladder neck strictures.

Methods

Laser ablation tests were conducted with 250-μm-core and 425-μm-core germanium oxide fibers in direct contact with urological soft tissue samples. A total of 500 pulses was delivered to the tissue. Pre- and post-ablation fiber output energies were measured to determine whether any damage occurred to the fiber tip. An optical microscope was used to analyze the output ends of the germanium fibers for evidence of fiber tip degradation after contact tissue ablation.

Fiber Damage Thresholds

The fiber damage thresholds for the soft tissue studies were 4 mJ (7 J/cm^2) and 9 mJ (6 J/cm^2) for the 250 μm and 425 μm fibers, respectively (Figure 5). These values are above the threshold for perforating samples of ureteral tissue, 2 mJ (4.1 J/cm^2) and 5.1 mJ (3.7 J/cm^2), respectively. ***These results demonstrate that the germanium oxide fiber is capable of ablating soft tissues without fiber tip damage. However, the fiber is limited to operation at relatively low laser energies during contact tissue ablation, which may not be practical for clinical applications requiring rapid and efficient tissue ablation.***

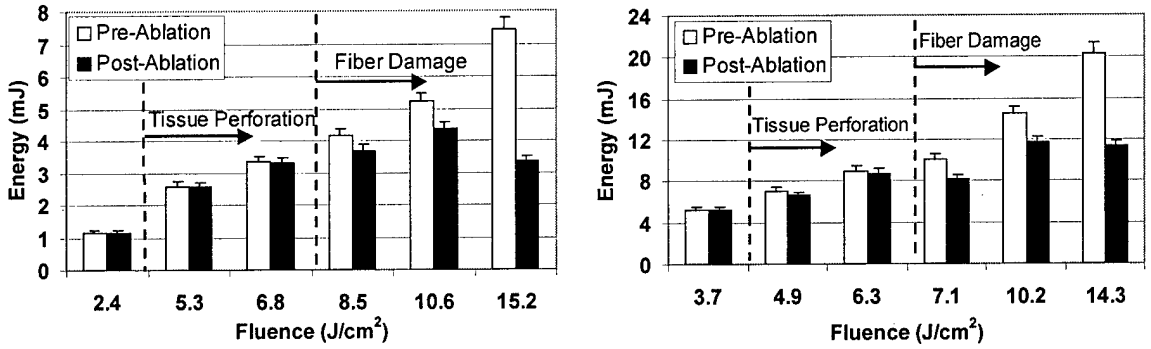

(a) 250 μm fiber **(b)** 425 μm fiber

Figure 5. Germanium fiber damage thresholds for (a) 250-μm-core fibers, and (b) 425-μm-core fibers, placed in direct contact with soft tissue. A total of 500 pulses were delivered with a pulse length of 70 μs and repetition rate of 10 Hz. Error bars signify a ± 5% variation in pulse to pulse energy stability.

Microscopic Analysis of Fiber Tips

The primary mechanism of germanium fiber damage during contact tissue ablation is melting of the fiber tip due to the high ablative temperatures. Figure 6 shows the fiber tips at different stages of meltdown, beginning with a normal tip surface, then particle formation, cracking and charring, and finally catastrophic meltdown with crystalline formation. During these phases, the fiber output energy also steadily dropped.

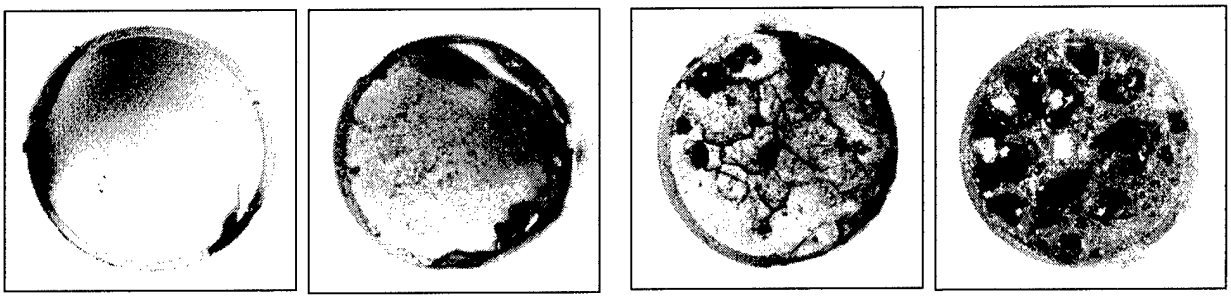

(a) **(b)** **(c)** **(d)**

Figure 6. Mechanism of germanium oxide fiber tip damage when tested in contact with tissue. (a) normal fiber tip, (b) particulate formation on the fiber tip, (c) cracking and charring, and (d) crystalline formation. The progressive deterioration is due to melting of the fiber tip when in contact with the tissue during high-temperature tissue ablation. Fiber tip damage was not observed during non-contact ablation studies. The parameters were: 425-μm-core fiber, 10 mJ/pulse, 70-μs-pulse duration, 10 Hz pulse repetition rate, and a total of 500 pulses.

Task 2.b. Design Side-Firing Laser Fibers for Incision of Urethral Wall.

We did not complete this task. After performing extensive studies characterizing the germanium fibers, we found that it was not necessary to design side-firing fibers to complete the other goals of the grant. The endoscopes and germanium fibers used in this research have proven to be sufficiently flexible for our application. If there becomes a crucial need for side-firing fibers, then we will develop them in Year 2 of the grant.

Task 2.c. Build Hybrid Optical Fibers that are both Flexible and Robust

Problem: Studies performed in Task 2.a. showed that the germanium fiber is limited to operation at very low Erbium:YAG laser energies when the fiber tip is in contact with tissue. This is a problem for laser treatment of strictures, which may require application of higher pulse energies for rapid and efficient incision of the urethra and bladder neck.

Solution: The goal of this study is to test a hybrid optical fiber with the Erbium:YAG laser, which combines the high-power transmission and flexibility of the germanium oxide fiber with the robust and biocompatible low-OH silica fiber tips currently in clinical use with the Holmium:YAG laser. This study demonstrates that long hybrid fibers are capable of being assembled with a simple process that reduces many of the limitations associated with current mid-IR optical fibers, and that sufficient Er:YAG laser energy can be transmitted through these fibers during insertion into a flexible endoscope for use in applications requiring soft tissue ablation.

Hybrid Germanium / Silica Fiber Assembly

The hybrid fiber consisted of a 1-cm-long, 550-μm-core, low-OH silica fiber tip attached to either a 350-μm- or 425-μm germanium trunk fiber. For the initial fiber preparation, the germanium fiber jacket was softened using chemical treatment (1-methyl-2-pyrrolidinone at 150 °C for 2 min. then isopropanol for 3 min.) and then stripped with a razor blade. The germanium and silica fibers were polished with rough 600-grit and then fine 5-micron sandpaper. The fibers were then aligned under a microscope using a laboratory-constructed mechanical setup.

Several different methods of attachment were explored (Figure 7). First, index-matching UV-cured optical epoxy (Norland, New Brunswick, NJ) was applied with a syringe needle either around the fibers or at the fiber interface (n = 10 fibers). Second, 30-gauge PTFE heat shrink tubing (normal ID=850 μm, shrunk ID=375 μm, wall thickness = 150 μm, length = 5 mm) was shrunk around the germanium/silica fiber interface using a heat gun (n = 10 fibers). The PTFE tubing (Small Parts, Miami Lakes, FL) also served the purpose of acting as a biocompatible jacket surrounding any exposed germanium fiber. Third, stainless steel hypodermic tubing (Small Parts, ID=0.675 mm, OD=1.05 mm) was used to align the fibers (n = 5 fibers). Fourth, glass capillary tubing (VitroCom, Mountain Lakes, NJ, ID=0.7 mm, OD=0.87 mm) was used for fiber attachment. Two attachment methods were explored: the fibers in contact at the interface (n = 10 fibers) or with an air gap (~200 μm) at the interface (n = 10 fibers).

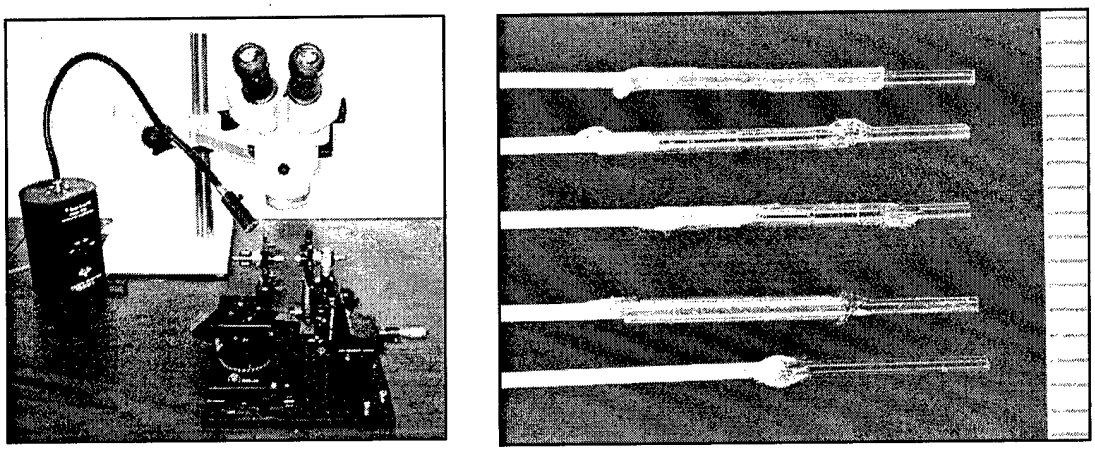

(a) (b)

Figure 7. (a) Experimental setup used to assemble the hybrid fibers. (b) Image of the germanium / silica hybrid fibers assembled using 5 different methods: (1) heat-shrink tubing, (2) glass capillary tubing, (3) glass tubing with an air gap at the fiber interface, (4) stainless steel hypodermic tubing, and (5) UV-cured optical epoxy. For all of the methods, an approximately 1 cm-long, 550-μm-core, low-OH silica tip was attached to a 425-μm-core germanium trunk fiber. Ball-shaped glue drops are present in Figures b-e at the interface between the yellow germanium jacket and the conduit material and at the interface between the silica tip and the conduit. The ruler lines = 1 mm.

To overcome the limitations of the germanium fiber for contact tissue ablation, a hybrid fiber consisting of a short low-OH silica fiber tip was attached to the germanium trunk fiber using several different methods. Table 2 shows the average output energy transmitted through the fiber for each of these methods before a drop in output energy was observed due to damage at the germanium / silica interface. The damage threshold for the germanium fiber without silica tip during contact soft tissue ablation is also included for comparison. ***Using the heat-shrink tubing method, hybrid fiber output energies measured 180 ± 30 mJ before fiber damage was observed (n=10), a 20-fold increase over the bare germanium fibers which damaged at only 9 mJ in contact with tissue (n=3).***

Table 2. Comparison of results for different methods used to construct germanium / silica hybrid fibers.

Assembly Method[a]	Maximum Pulse Energy (mJ)	N
Germanium tip only[b]	9 ± 1	3
Silica tip attached with:		
UV-cured epoxy	10 ± 5	10
Steel hypodermic tubing	109 ± 47	10
Glass capillary tubing:		
with air gap at interface	104 ± 38	10
without air gap at interface	139 ± 49	10
Heat-shrink tubing	180 ± 30	10

[a] All fibers were constructed using a 425-μm-core germanium trunk fiber and a 1-cm-long, 550-μm-core silica fiber tip. The fibers were tested using an Er:YAG laser with a 220 μs laser pulse length at 3 Hz.

[b] Values for the germanium fibers without silica tip represent maximum pulse energies achieved during contact soft tissue ablation. No problems were encountered during non-contact ablation.

Fiber Bending Tests

Preliminary fiber bending tests were conducted with germanium and sapphire optical fibers, ranging in core diameter from 150 – 500 μm. The fibers were inserted into a 15 Fr flexible cysto-urethroscope with a 7 Fr working channel. Basic fiber testing was performed to determine whether the fiber could withstand high mechanical stress under tight bending conditions and whether the fiber presence hindered maximum deflection of the scope. Peak Er:YAG energy transmission through the hybrid fibers was then measured for both straight and bent configurations.

Earlier tests showed that the sapphire optical fibers were more robust than the germanium fibers, as evidenced by the difference in their melting temperatures (2030 °C versus 680 °C) and the absence of fiber tip damage during contact soft tissue ablation. However, the sapphire fiber was not pursued further because both 250-μm- and 425-μm-core sapphire fibers suffered multiple fractures upon insertion into the flexible cysto-urethroscope under tight bending conditions (Table 3). While the 425-μm-core germanium fibers also fractured upon repeated bending, the 150-μm-, 250-μm-, and 350-μm-core germanium fibers suffered no mechanical damage under similar test conditions. Figure 8 shows a 350-μm-core germanium oxide fiber inserted through the 7 Fr working channel of a 15 Fr flexible cysto-urethroscope. The scope was deflected at a maximum angle corresponding to a bend radius of approximately 15 mm with and without the fiber inserted.

Table 3. Bending tests performed using a 15 Fr flexible cysto-urethroscope with 7 Fr working channel and ~ 15 mm bend radius.

Fiber Type / Core Size	**Minimum Bend Radius[a]**	**Flexible Scope Breaking Test**
Sapphire		
150 μm	20 mm	Passed
250 μm	30 mm	Failed
325 μm	60 mm	Not tested
425 μm	80 mm	Failed
Germanium Oxide		
150 μm	5 mm	Passed
250 μm	10 mm	Passed
350 μm	15 mm	Passed
425 μm	25 mm	Failed
500 μm	40 mm	Failed

[a] Minimum bend radius values are taken from commercial literature (www.photran.com and www.infraredfibersystems.com).

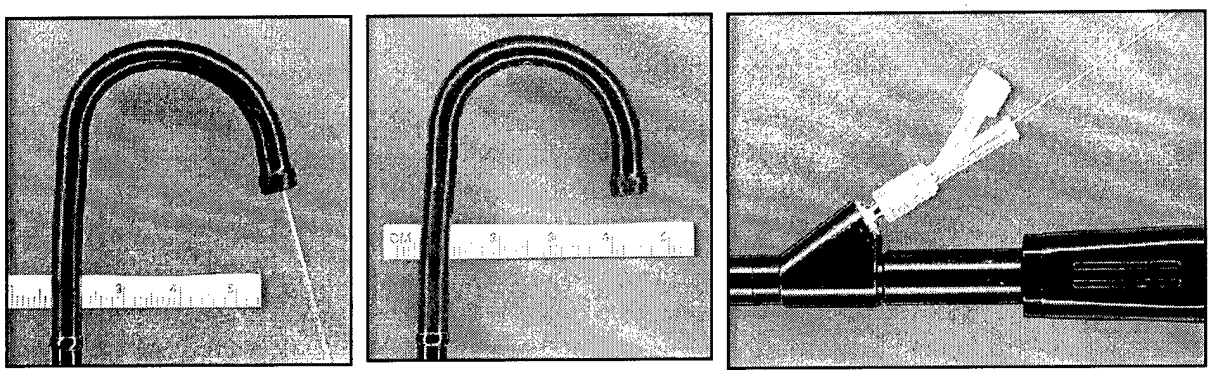

(a) (b) (c)

Figure 8. Images of a 350-μm-core germanium / silica hybrid fiber inserted through a 15 Fr flexible cysto-urethroscope with a 7 Fr working channel. (a) The fiber is bent to a ~ 15-mm bend radius without breaking under maximum scope deflection. (b) Maximum deflection of the scope without fiber present also corresponds to a ~ 15-mm bend radius, demonstrating that the fiber does not hinder scope deflection. (c) The fiber is successfully inserted at a 30-degree angle into the working channel.

Both the 350/550 and 425/550 germanium/silica hybrid fibers showed a significant decrease in energy output when bent to just above their minimum bending radius, 15 mm for the 350 μm trunk fiber and 25 mm for the 425 μm trunk fiber (Table 4). The damage mechanism was usually observed as sparking at the germanium/silica fiber interface, resulting in a melting of the germanium surface at the fiber interface, and noted as an immediate loss in energy greater than 5%. The difference in results between the 250-, 350- and 425-μm trunk fibers can be explained in part by the difference in the cross-sectional area at the germanium fiber tip. Assuming the melting temperature of the germanium fiber tip at the interface is the limiting factor, the maximum fluence that the interface can handle before melting is a function of both energy and fiber diameter. Thus, a larger trunk fiber diameter transmits greater energy, as observed in Table 3.

Table 4. Damage thresholds during germanium / silica fiber bending tests.

Fiber Core (μm) (Trunk / Tip)	**Maximum Energy (mJ)** Straight	Bent	**Bend Radius (mm)**	**N**
425 / 550	180 ± 30	82 ± 20	30	10
350 / 550	93 ± 13	65 ± 20	20	10
250 / 365	27 ± 8	28 ± 9	20	8

Overall, our results show that by adding a robust silica fiber tip to the germanium fiber, fiber output energies may be increased to 180 ± 30 mJ (76 ± 13 J/cm^2) and 82 ± 20 mJ (35 ± 9 J/cm^2), in straight and tight bending configurations, respectively, without fiber damage. This represents a 20-fold increase over the 9 mJ (6 J/cm^2) peak energy achieved during testing of the bare germanium fiber in contact with soft tissue during Task 2.a (Figure 5b). These results demonstrate that the hybrid germanium / silica fiber transmits sufficient energy for contact soft tissue ablation through a flexible endoscope.

KEY RESEARCH ACCOMPLISHMENTS

- Determined the energy threshold for Erbium:YAG laser ablation of urethral tissues.

- Constructed a chart measuring tissue removed per a laser pulse as a function of laser energy and pulse duration. This chart is important because during clinical studies it will provide the urologist with a method for choosing and predicting how deep to make the laser incision, based on the laser energy level and number of laser pulses delivered to the tissue. Thus, a laser incision in the scar tissue can be made without cutting too deep into healthy tissue.

- Decreased the peripheral thermal damage zone in urethral tissue caused by the Erbium laser by a factor of 2, from 30-60 μm to 15-30 μm. For comparison, the Holmium laser currently used in urology for incision of urethral and bladder neck strictures causes a minimum of 300-400 μm of thermal damage. Thus, our Erbium laser is 10-20 times more precise than the Holmium laser.

- Increased the rate of Erbium laser tissue cutting rate by a factor of 2, by reducing the laser pulse length from 220 to 70 μs. This will result in more rapid and efficient tissue cutting for clinical use.

- Determined the damage threshold and damage mechanism for the germanium optical fibers when used in contact mode for tissue ablation. This will allow the urologist to operate the laser at laser parameters that provide rapid and precise incision of tissue, without concern about permanently damaging the optical fiber delivery system.

- Constructed hybrid germanium / silica optical fiber delivery system capable of being used with flexible endoscopes for laser incision of strictures. Damage threshold of the hybrid fibers was measured to be 20 times greater than that of conventional germanium oxide fibers alone, making contact fiber optic tissue cutting feasible.

- Determined the transmission losses of the hybrid germanium / silica fibers when used in a bent configuration. These studies define the limits of the fiber when used in extreme bending configurations in flexible scopes, thus avoiding fibers from beraking and permanently damaging the endoscope.

REPORTABLE OUTCOMES

Manuscripts

1. **Fried NM**, Tesfaye Z, Ong AM, Rha KH, Hejazi P. Optimization of the erbium:YAG laser for precise incision of ureteral and urethral tissues: in vitro and in vivo results. Lasers in Surgery and Medicine 33:108-114, 2003.

2. Chaney CA, Yang Y, **Fried NM**. Hybrid germanium / silica optical fibers for endoscopic delivery of Erbium:YAG laser radiation. Lasers in Surgery and Medicine 34(1):5-11, 2004.

3. **Fried NM**, Tesfaye Z, Ong AM, Rha KH, Hejazi P. Variable pulsewidth Erbium:YAG laser ablation of the ureter and urethra in vitro and in vivo: optimization of the laser fluence, pulse duration, and pulse repetition rate. Proc. SPIE: Lasers in Urology. In Press.

4. Chaney CA, Yang Y, **Fried NM.** Assembly and testing of germanium / silica optical fibers for flexible endoscopic delivery of Erbium:YAG laser radiation. Proc. SPIE: Lasers in Urology. In Press.

Abstracts

1. **Fried NM**, Ong AM, Rha KH, Tesfaye Z, Hejazi P. Erbium:YAG laser incision of the ureter and urethra: optimization of the laser parameters. Journal of Endourology 17(9):832, 2003.

2. **Fried NM**, Chaney CA. Hybrid germanium / silica optical fibers for flexible endoscopic delivery of high-power Erbium:YAG laser radiation. Journal of Endourology 17 (Suppl. 1):A40, 2003.

CONCLUSIONS

In the first year of this research project, we have accomplished several objectives. First, we demonstrated that the Erbium:YAG laser is more precise than the Holmium:YAG laser (currently the laser of choice in urology) for incision of urethral tissue. The Erbium laser produces a factor of 10-20 times less peripheral thermal damage to adjacent healthy tissue than does the Holmium laser (15-30 μm for the Erbium versus 300-400 μm for the Holmium laser). This result is important because the amount of thermal damage is believed to be a major factor in causing tissue scarring during wound healing and stricture recurrence.

Second, we constructed a novel optical fiber delivery system for delivering the Erbium laser radiation through either a rigid or flexible endoscope for use in minimally invasive laser treatment of strictures. This hybrid optical fiber combines the high laser power transmission of the germanium oxide fiber optic material used as a "trunk" fiber with a robust fiber tip made of silica, and able to withstand high laser powers without damaging.

In the second year of this research grant, we will continue to improve our fiber optic delivery system. Then we plan to conduct in vivo animal studies in a pig model to quantify the wound healing process after Erbium laser incision. Acute studies will be conducted to verify that our in vivo results are comparable to the results of the ex vivo tissue studies described here. Then, chronic wound healing studies will be conducted to determine whether the minimal peripheral thermal damage caused by the Erbium laser will translate into significant scarring. Acute and chronic studies will also be conducted with the Holmium laser as a control arm for comparison with the Erbium laser.

REFERENCES

1. R. V. Clayman, E. M. McDougall, S. Y. Nakada SY, "Endourology of the upper urinary tract: percutaneous renal and ureteral procedures," In: P. C. Walsh, A. B. Retik, E. D. Vaughan, A. J. Wein, eds. Campbell's Urology, 7th ed., Vol. 3, Philadelphia: WB Saunders. Pp. 2853-2863, 1998.

2. G. H. Jordan, S. M. Schlossberg, C. J. Devine, "Surgery of the penis and urethra," P. C. Walsh, A. B. Retik, E. D. Vaughan, A. J. Wein, eds. Campbell's Urology, 7th ed., Vol. 3, Philadelphia: WB Saunders, pp. 3341-3347, 1998.

3. M. A. Rosen, P. A. Nash, J. E. Bruce, J. W. McAninch, "The actuarial success rate of surgical treatment of urethral strictures," *J. Urol.*, vol. 151, p. 360A, 1994.

4. P. Albers, J. Fichtner, P. Bruhl, S. C. Muller, "Long-term results of internal urethrotomy," *J. Urol.*, vol. 156, pp. 1611-1614, 1996.

5. A. Benchekroun, A. Lachkar, A. Soumana, M. H. Farih, Z. Belahnech, M. Marzouk, M. Faik, "Internal urethrotomy in treatment of urethral stenoses (longterm results)," *Ann. Urol. (Paris)*, vol. 32, pp. 99-102, 1998.

6. C. F. Heyns, J. W. Steenkamp, M. L. De Kock, P. Whitaker, "Treatment of male urethral strictures: is repeated dilation or internal urethrotomy useful?" *J. Urol.*, vol. 160, pp. 356-358, 1998.

7. **N. M. Fried**, "Potential applications of the Erbium:YAG laser in endourology," *J. Endourol.*, vol. 15(9), pp. 889-894, 2001.

8. **N. M. Fried**, G. M. Long, "Erbium:YAG laser ablation of urethral and ureteral tissues," *Proc. S.P.I.E.: Lasers in Urology*, vol. 4609, pp. 122-127, 2002.

9. **N. M. Fried**, Z. Tesfaye, A. M. Ong, K. H. Rha, P. Hejazi, "Optimization of the Erbium:YAG laser for precise incision of ureteral & urethral tissues: in vitro & in vivo results," *Lasers Surg. Med.*, vol. 33, pp. 108-144, 2003.

10. C. A. Chaney, Y. Yang, **N. M. Fried**, "Hybrid germanium / silica optical fibers for endoscopic delivery of Erbium:YAG laser radiation" *Lasers Surg. Med.*, vol. 34(1), pp. 5-11, 2004.

11. J. A. Harrington, "A review of infrared fibers," http://irfibers.rutgers.edu/ir-rev-index.html. OSA Handbook, Vol. III, McGraw-Hill. Editor, Michael Bass, 2000.

12. G. N. Merberg, "Current status of infrared fiber optics for medical laser power delivery," *Lasers Surg. Med.*, vol. 13, pp. 572-576, 1993.

13. Personal communication - Alex Tchap, Infrared Fiber Systems, Silver Spring, MD.

APPENDICES

Copies of all manuscripts and abstracts from this research are attached to this report.

Lasers in Surgery and Medicine 33:108–114 (2003)

Optimization of the Erbium:YAG Laser for Precise Incision of Ureteral and Urethral Tissues: In Vitro and In Vivo Results

Nathaniel M. Fried, PhD,[1]* Zelalem Tesfaye, MS,[1] Albert M. Ong, MD,[1] Koon H. Rha, MD, PhD,[1] and Pooya Hejazi, MS[2]

[1]*Department of Urology, Johns Hopkins Medical Institutions, Baltimore, Maryland 21224*

[2]*Department of Electrical Engineering and Computer Science, Johns Hopkins University, Baltimore, Maryland 21218*

Background and Objectives: Tissue damage during endoscopic treatment of urethral and ureteral strictures may result in stricture recurrence. The Erbium:YAG laser ablates soft tissues with minimal peripheral damage and may be a promising alternative to cold knife and Holmium:YAG laser for precise incision of urological strictures.

Study Design/Materials and Methods: Optimization of the Er:YAG laser was conducted using ex vivo porcine ureteral and canine urethral tissues. Preliminary in vivo studies were also performed in a laparoscopic porcine ureteral model with exposed ureter. Laser radiation with a wavelength of 2.94 μm, pulse lengths of 8, 70, and 220 microseconds, output energies of 2–35 mJ, fluences of 1–25 J/cm^2, and pulse repetition rates of 5–30 Hz, was delivered through 250-μm and 425-μm core germanium oxide optical fibers in direct contact with tissue.

Results: Ex vivo perforation thresholds measured 2–4 J/cm^2, with ablation rates of 50 μm/pulse at fluences of 6–11 J/cm^2. In vivo perforation thresholds were approximately 1.8 J/cm^2, with the ureter perforated in less than 20 pulses at fluences greater than 3.6 J/cm^2. Peripheral thermal damage in tissue decreased from 30 to 60 μm to 10–20 μm as the laser pulse length decreased from 220 to 8 microseconds. Mechanical tissue damage was observed at the 8 microseconds pulse duration.

Conclusions: The Er:YAG laser, operating at a pulse duration of ~70 microseconds, a fluence greater than ~4 J/cm^2, and a repetition rate less than 20 Hz, is capable of rapidly incising urethral and ureteral tissues with minimal thermal and mechanical side-effects. Lasers Surg. Med. 33:108–114, 2003. © 2003 Wiley-Liss, Inc.

Key words: stricture; urethra; ureter; Erbium; Holmium; laser; ablation; incision

INTRODUCTION

Urethral and ureteral strictures occur as a result of trauma to the tissues caused during surgery, for example, transurethral resection of the prostate, radical retropubic prostatectomy, minimally invasive thermal therapies of the prostate, and endosurgery of the upper urinary tract [1,2]. Scarring and narrowing of the lumen may then lead to incontinence and/or urinary tract infection.

Several techniques are currently available for minimally invasive treatment of urological strictures, including balloon dilation, cold knife incision, electrocautery, and Holmium:YAG laser incision [1,2]. Balloon dilation and cold knife incision are the preferred endourologic methods of treatment for strictures, but they have widely variable success rates ranging from 20 to 80% [3–6]. Balloon dilation is ineffective in strictures where there is scar tissue present, and balloon expansion may cause further stress-induced damage to the urethral or ureteral wall. Cold knife incision may cause mechanical damage to the wall during cutting, resulting in stricture recurrence. Electrocautery and Ho:YAG laser produce significant thermal damage in adjacent healthy tissue, which may induce further scar formation and re-stricture. None of these methods are ideal for treating strictures and it is often necessary to repeatedly dilate or incise the stricture. Studies have shown, however, that multiple dilations or incisions in patients with complicated strictures do not provide increased benefit, leaving these patients without an effective method for treating recalcitrant scarring and secondary complications of voiding dysfunction and urinary incontinence [2].

A variety of lasers have been used for treating strictures over the past 20 years [7], including CO_2 [8], argon [9,10], KTP [11,12], Nd:YAG [13–16], Ho:YAG [17–24], and excimer [25] lasers. Outcomes of laser therapy have been sub-optimal due to stricture recurrence, presumably caused by excessive thermal damage to adjacent tissue

Contract grant sponsor: NIH Phase I SBIR awarded; Contract grant number: 1R43 EY13889-01; Contract grant sponsor: National Kidney Foundation of Maryland; Contract grant sponsor: Department of Defense Prostate Cancer Research Program; Contract grant number: PC020586.

*Correspondence to: Nathaniel M. Fried, PhD, Department of Urology, Johns Hopkins Bayview Medical Center, 4940 Eastern Avenue, Building A, Room 347c, Baltimore, MD 21224.
E-mail: nfried@jhmi.edu

Accepted 8 May 2003
Published online in Wiley InterScience (www.interscience.wiley.com).
DOI 10.1002/lsm.10205

and subsequent scar formation. Recently, the Ho:YAG laser has become the laser of choice in urology, because of its multiple uses, including treatment of urinary tract stones, strictures, and superficial bladder tumors. The Ho:YAG laser, however, produces an average of 300 μm of residual peripheral thermal damage during soft tissue ablation, and therefore, may not be optimal for precise incision of strictures. Excessive thermal damage during stricture treatment may increase the probability of stricture recurrence, as evidenced by the existence of animal models for thermal induction of strictures [26,27].

Previous studies have shown that the Er:YAG laser efficiently ablates soft tissues with minimal peripheral thermal damage. The Er:YAG laser is currently being used in several medical fields, including dermatology, dentistry, and ophthalmology which require precise ablation of delicate tissues. Recent experimental studies have also explored the use of the Er:YAG laser in urology for lithotripsy [28,29], and initial results in our laboratory have shown that the Er:YAG laser may also be promising for treatment of strictures [30,31]. The goal of this study is to optimize the Er:YAG laser parameters for rapid and precise incision of urethral and ureteral tissues.

MATERIALS AND METHODS

Laser Parameters

An Erbium:YAG laser (SEO 1-2-3, Schwartz Electro-optics, Orlando, FL) operating at a wavelength of 2.94 μm was connected to a variable pulsewidth laser power supply (Model 8800V, Analog Modules, Longwood, FL), producing laser pulse lengths from 1 to 220 microseconds. The laser radiation was externally focused with a 50-mm-focal-length calcium fluoride lens into either 250 or 425-μm-core germanium oxide optical fibers (Infrared Fiber Systems, Silver Spring, MD). A green aiming beam (5 mW, $\lambda = 532$ nm, Intelite, Minden, NV) was coupled into the fiber for alignment purposes.

The laser was operated at pulse repetition rates of 5–30 Hz, pulse energies of 2–35 mJ, and fluences of 1–25 J/cm^2. The laser energy was measured using a pyroelectric detector (Gentec ED-200, Ste.-Foy, Que.), and the pulse duration was measured using a photovoltaic infrared detector (PD-10.6, Boston Electronics, Brookline, MA). Figure 1 shows the temporal beam profiles from 1 to 220 microseconds. Ablation rate studies were performed at only the 8, 70, and 220 microsecond pulse lengths, because there was insufficient output energy for tissue ablation at the 1 microsecond pulse duration (<0.2 mJ/pulse). The 8 microseconds pulse consisted of a packet of two micropulses, and an output energy of up to 10 mJ, sufficient for tissue ablation at low pulse repetition rates of less than 10 Hz. The 70 microseconds pulse duration produced enough output energy for laser ablation studies at pulse repetition rates of less than or equal to 30 Hz. Thermal lensing effects in the laser rod prevented operation of the laser at higher pulse repetition rates without a significant reduction of energy output to below tissue ablation thresholds.

In Vitro Tissue Preparation

Fresh ureteral tissue samples were removed from adult female pigs (100 kg) directly after sacrifice at the local slaughterhouse (Mt. Airy Locker Company, Mt. Airy, MD). Fatty tissue was shaved from the ureter with a #10 scalpel blade, the tissue was spatulated, cut into 1 × 1 cm samples, stored in normal saline, and refrigerated for use within 24 hours. Fresh prostatic urethral tissue samples were obtained from male dogs (25–30 kg) after sacrifice for unrelated experiments at the Johns Hopkins Medical School. The posterior urethra was dissected from the prostate, spatulated, sectioned into 1 × 1 cm samples, stored in saline, and refrigerated.

For the ablation measurements, tissue samples were sandwiched between microscope and plexiglass slides to a fixed thickness (350 ± 50 μm), and the optical fiber tip positioned in contact with the sample through 2-mm-diameter holes drilled in the front plexiglass holder. The tissue samples were kept hydrated with saline using a syringe during the ablation experiments. The samples were placed in front of a pyroelectric detector, and the number of pulses required to perforate each sample was measured. The pyroelectric detector was connected to an oscilloscope (Model TDS210, Tektronix, Beaverton, OR) and signals as small as 0.1 J/cm^2 could be detected indicating perforation of the tissue.

In Vivo Animal Experiments

All animal protocols were reviewed and approved by the Animal Care and Use Committee at the Johns Hopkins University School of Medicine. A total of four female pigs (30–45 kg, Archer Farms, Belcamp, MD) were pretreated with acepromazine 0.39 mg/kg IM and ketamine 2 mg/kg IM. After the animals were sedated, intravenous access was obtained and normal saline administered as a 5 ml/cc bolus followed by a maintenance rate of 1.5 ml/kg/hour. Intravenous propofol was administered for anesthesia. After adequate depth of anesthesia, the animal was positioned and laparoscopic ports were placed in the standard 3-port configuration, using a Visiport (US Surgical Corp., Norwalk, CT) for initial access. Using laparoscopic instrumentation, the ipsilateral ureter was identified and isolated, taking care to avoid excessive dissection and skeletonization. The distal ureter was ligated and transected close to the bladder. A small incision was made in the body wall and the ureter brought external to the body. The ureter was then spatulated and marked with 6-0 prolene sutures. The laser fiber was placed on the ureteral lumen, and the number of laser pulses required to perforate the ureter was recorded. An average of 12 perforations were made in each ureter, spaced approximately 5 mm apart, and marked by sutures on each side. Perforation was confirmed by several indicators, including penetration of the green aiming beam, an audible change in the acoustic ablation signal during ablation, and later by histologic analysis.

Data Analysis

A minimum of six perforations were made for each set of laser parameters. Only three measurements were made

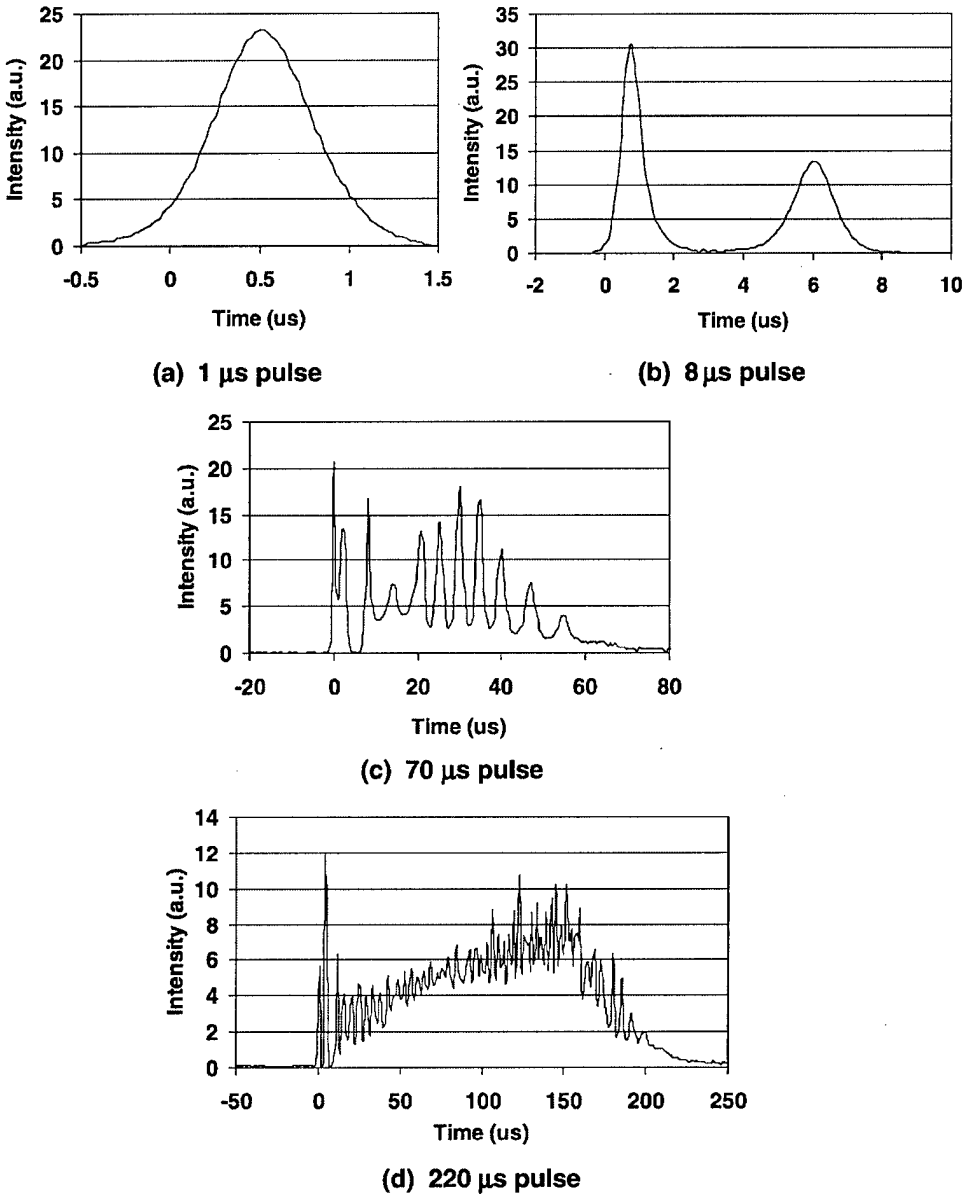

Fig. 1. Temporal pulse profiles for the Er:YAG laser operated with pulse lengths from 1 to 220 microseconds.

for energies below the perforation threshold. For the ex vivo tissue studies, ablation rates (μm/pulse) were defined as the sample thickness divided by the average number of pulses required to perforate the sample and recorded as the mean ± standard deviation (SD). Irradiation was stopped if perforation was not achieved after 100 laser pulses. The optical fiber tip was kept fixed in contact with the tissue during the ex vivo tissue experiments. For the in vivo studies, the optical fiber was advanced during ablation. The in vivo ablation results were recorded in terms of the number of pulses required to perforate the ureteral wall because it was not possible to control for the tissue wall thickness across different ureters and animals.

RESULTS

Ablation Rates

The Er:YAG ablation rates are shown in Figure 2 for the ex vivo tissue experiments. Perforation of the 350-μm-thick ureteral tissue samples was achieved at fluences of approximately 3–5 J/cm^2 and pulse energies of 1.5–2.5 mJ, without advancing the fiber into the tissue during ablation. There was an almost twofold increase in the ablation rate

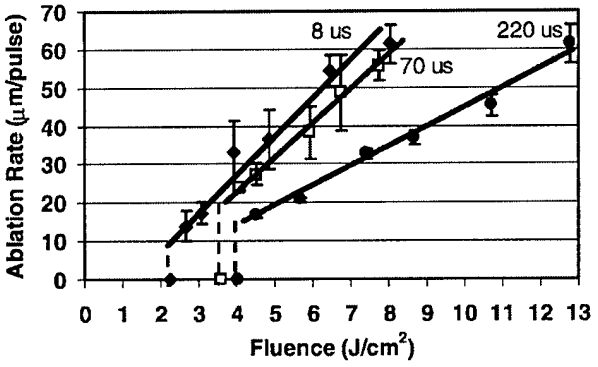

Fig. 2. Er:YAG ablation rates for ex vivo ureter tissue using laser pulse lengths of 8, 70, and 220 microseconds, and plotted as a function of laser fluence. Bars signify mean values ± SD (n = 6). Note that the perforation threshold decreases as the laser pulse is decreased, and ablation is also more efficient.

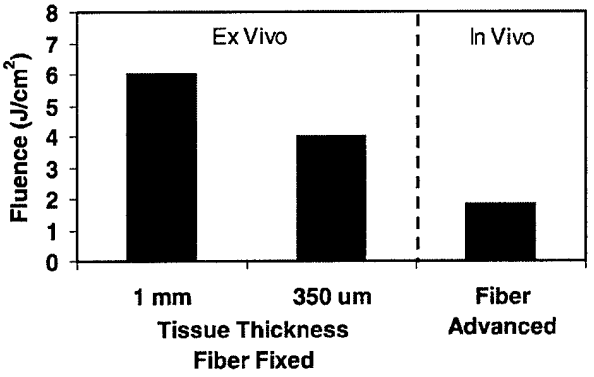

Fig. 4. Perforation threshold for Er:YAG ablation of ureteral tissue measured using 1-mm-thick and 350-μm-thick tissue samples and a fixed fiber tip, compared with advancement of the fiber tip during in vivo ablation studies. All values correspond to a laser pulse duration of ~220 microseconds, for comparison.

for a given fluence when reducing the laser pulse duration from 220 to 70 microseconds. Tissue removal rates increased from 4 microns per a J/cm^2 to 7 microns per a J/cm^2. Reducing the pulse duration further to 8 microseconds, however, produced only a minor improvement in the ablation rate, at the expense of much lower laser energy output and peripheral mechanical tissue damage, as described below.

The in vivo ablation results are shown in Figure 3, plotted as the number of laser pulses to perforate the ureter, with the fiber advanced into the tissue during ablation. The ureteral wall was perforated with less than 20 pulses at a fluence of 3.6 J/cm^2 for all of the laser pulse lengths tested. At the lowest fluence of 1.8 J/cm^2, near the perforation threshold, the shorter laser pulse lengths were observed to be more efficient. This perforation threshold was lower than that observed for the ex vivo tissue experiments using thick or thin tissue samples, as shown in Figure 4.

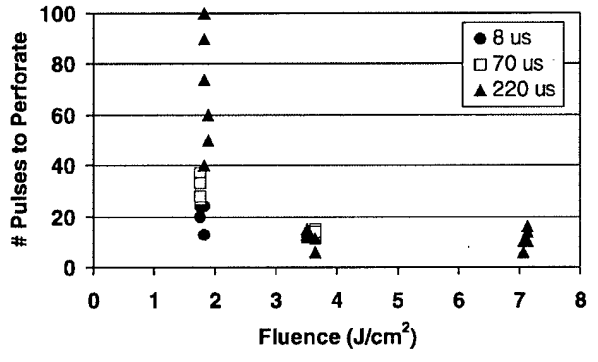

Fig. 3. Er:YAG results for in vivo ureter ablation as a function of laser pulse length and fluence. The perforation threshold is approximately 1.8 J/cm^2, based on the increase in the number of pulses for perforation, and the large spread in the data points.

Thermal Damage Measurements

Histological measurements of thermal damage were conducted as a function of laser pulse duration. The results for the ex vivo tissue studies are shown in Figure 5. When the Er:YAG laser was operated in its normal long pulse mode (220 microseconds pulse length), a thermal damage zone of 30–60 μm was observed. Shortening the laser pulse to 70 microseconds resulted in a reduction of the thermal damage to 15–30 μm. The shortest laser pulse, measuring 8 microseconds, further reduced the thermal damage zone to 10–20 μm, but also resulted in a rougher, jagged cut, due to mechanical tissue-tearing effects caused by the laser pulses.

An ex vivo study was also performed to determine whether the thermal damage zone would increase with laser operation at higher pulse repetition rates, due to residual heat accumulation in the tissue with deposition of successive laser pulses. The pulse duration, energy per pulse, and total number of pulses delivered to the tissue were all kept constant at 70 microseconds, 10 mJ, and 20 pulses (total energy = 200 mJ), respectively, while the pulse repetition rate was varied from 10 to 30 Hz. The thermal damage zone increased as the laser pulse repetition rate increased, and a large increase in thermal damage was observed when the pulse repetition rate was increased from 20 to 30 Hz (Fig. 6).

The in vivo histological results are shown in Figure 7, for the intermediate, 70 microseconds pulse duration. The thermal damage zone of 10–20 μm is slightly less than the 15–30 μm of thermal damage observed in the ex vivo tissue studies for 70 microseconds pulse lengths and considerably less than the 30–60 μm of thermal damage observed for the long pulse mode of 220 microseconds.

DISCUSSION

Success rates in treating strictures vary widely from 20 to 80%, dependent on a variety of factors, including surgical

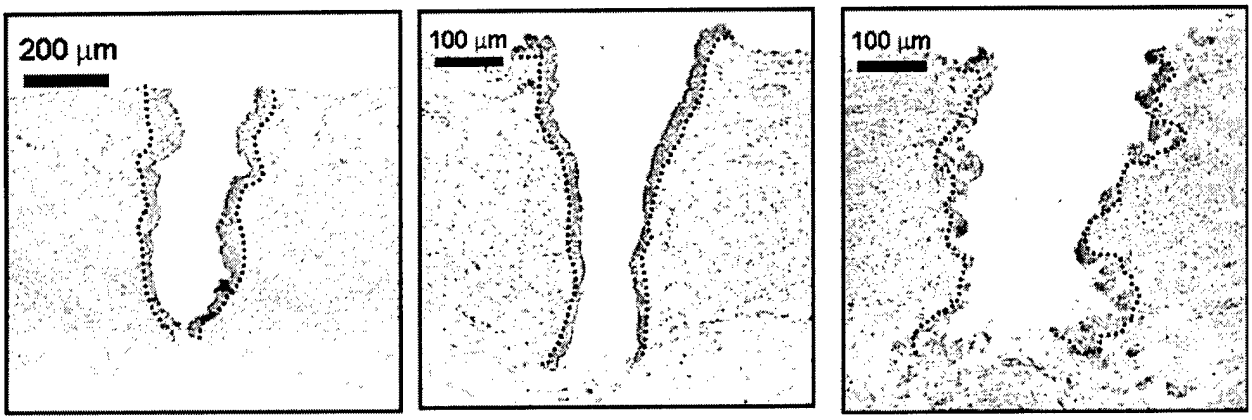

Fig. 5. Photomicrographs showing H&E stained histologic cross-sections of ureteral tissues ablated with the Er:YAG laser, ex vivo. Note that the thermal damage zone decreases as the laser pulse duration is decreased. Rough, jagged borders of the ablation crater produced by 8 microseconds laser pulses may be due to mechanical tissue-tearing caused during ablation. The dotted lines demarcate the border of the thermal damage zone.

technique and skill, type of stricture, scar tissue caused by previous treatment failures, patient follow-up and evaluation, and definition of stricture. While the use of the Ho:YAG laser has resulted in improved treatment of strictures, we hypothesize that the further reduction of peripheral thermal damage to the urethral or ureteral wall with Er:YAG laser incision may further improve these success rates. By operating at the 2.94 μm wavelength of the Er:YAG laser, and shortening the laser pulse length to approximately 70 microseconds, the thermal damage zone has been reduced to 10–20 μm, in vivo. This represents a 15–30-fold decrease in damage in comparison to the 300 μm of damage typically produced by the Ho:YAG laser, which is currently the laser of choice in urology.

Our results are similar to those of previous studies using the Er:YAG laser for ablation of other soft tissues. For example, reported threshold fluences of ablation for the long-pulse Er:YAG laser are 0.6–1.5 J/cm^2 for skin [32], ~2 J/cm^2 for aorta [33], ~1 J/cm^2 for retina [34], and ~1.8 J/cm^2 for the ureter reported here. Note that these low

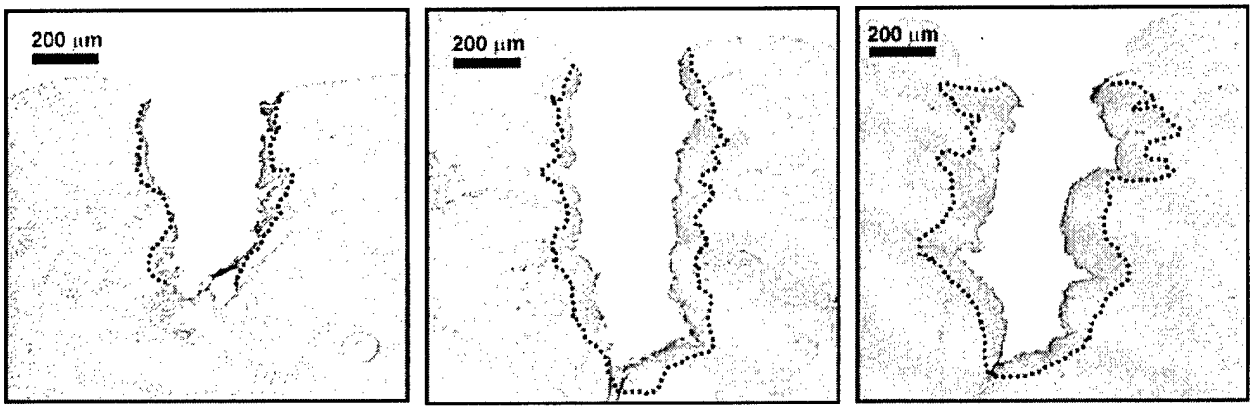

Fig. 6. Photomicrographs showing H&E stained histologic cross-sections of urethral tissues ablated with the Er:YAG laser, ex vivo, with varying laser pulse repetition rates of 10–30 Hz. Energy was kept fixed at 10 mJ/pulse with a total of 20 pulses (200 mJ) delivered to the tissue. Note that there is a large increase in the thermal damage zone from 20 to 30 Hz, due to residual heat accumulation in the tissue during ablation. The dotted lines demarcate the border of the thermal damage zone.

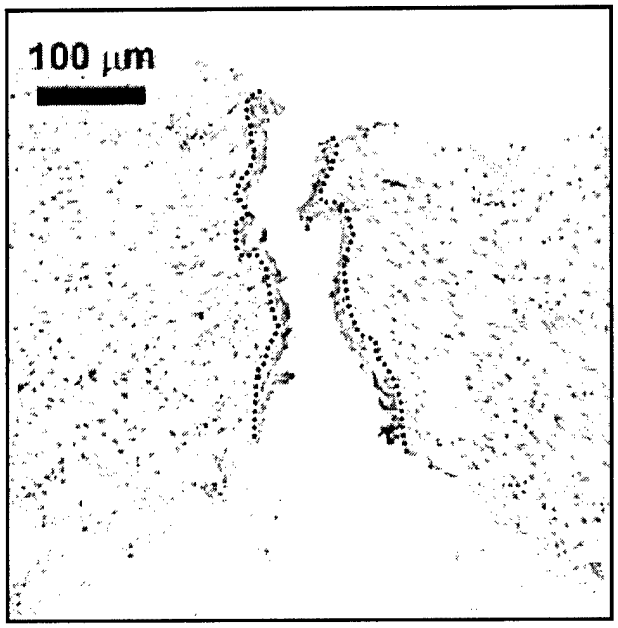

Fig. 7. Photomicrograph showing H&E stained histologic cross-section of ureteral tissue ablated with the Er:YAG laser, in vivo. The thermal damage zone measures 10–20 μm. The dotted lines demarcate the border of the thermal damage zone.

ablation thresholds also demonstrate that the Er:YAG laser is more efficient than the Ho:YAG laser, which has an ablation threshold of ~34 J/cm^2.

Thermal damage zones in other soft tissues for the long-pulse Er:YAG laser operated at low fluences (<25 J/cm^2) have been reported to be 10–40 μm for skin [35], 10–20 μm for aorta [35], 20–40 μm for cornea [35], <50 μm for trabecular tissue [36], 20–30 μm for retina [34], and 30–60 μm for ureter reported here. Mechanical tissue-tearing effects have also been observed in other tissues, for example, aorta and cornea [35], and at pulse lengths of 50 microseconds and shorter [36]. Although we did not observe any mechanical tissue damage at the 70 microseconds pulse length, the 8-microseconds-pulse-length showed evidence of tissue shredding consistent with that observed in these previous studies.

Problems with the fiber tip "sticking" to the tissue during contact tissue ablation with the Er:YAG laser have also been previously reported [37,38]. This phenomenon was explained by the presence of overheated tissue debris at the fiber tip. During our preliminary in vivo experiments, however, we did not observe any "sticking" effects during advancement of the fiber into the ureter. This may be due to the use of different laser parameters, optical fibers, and/or tissues, and needs to be further studied.

In general, lower perforation thresholds, higher ablation rates, and less thermal damage were observed when progressing from ex vivo to in vivo experiments. Several factors may have contributed to these differences. First, the ability to advance the optical fiber into the tissue during in vivo ablation studies resulted in lower perforation thresholds and higher ablation rates for a given fluence. This occurred because the fluence at the tissue surface was not diminished due to divergence of the laser radiation at the output end of the fiber tip. Second, the decreased thermal damage seen in vivo may also be due to the level of hydration maintained in the tissue and absence of tissue desication which can occur during ex vivo tissue experiments.

CONCLUSIONS

The Er:YAG laser, operating at a pulse duration of ~70 microseconds, a fluence greater than ~4 J/cm^2, and a repetition rate less than 20 Hz, is capable of rapidly incising urethral and ureteral tissues, in vivo, with minimal thermal and mechanical side-effects. The Er:YAG laser is more efficient than the Ho:YAG laser for cutting ureteral and urethral tissues, with perforation thresholds measuring 2 J/cm^2 versus 34 J/cm^2, respectively. The Er:YAG laser is also more precise than the Ho:YAG laser, with peripheral thermal damage zones measuring 10–20 μm versus 300 μm, respectively. Chronic animal wound healing studies are planned to quantify scarring induced during Er:YAG laser incision, and optimization of mid-infrared fiber optic delivery systems for endoscopic laser delivery has begun.

ACKNOWLEDGMENTS

We thank Paul Chaiseesiri for his help in preparing the histology, and Ken Levin, Dan Tranh, and Alex Tchap of Infrared Fiber Systems, for providing the optical fibers used in these experiments. This research was supported in part by the following grants and sponsors: laboratory start-up funding from the James Buchanan Brady Urological Institute; NIH Phase I SBIR awarded to Infrared Fiber Systems (Silver Spring, MD), Grant no. 1R43 EY13889-01; a Professional Development Award from the National Kidney Foundation of Maryland; and the Department of Defense Prostate Cancer Research Program, Grant no. PC020586.

REFERENCES

1. Clayman RV, McDougall EM, Nakada SY. Endourology of the upper urinary tract: Percutaneous renal and ureteral procedures. In: Walsh PC, Retik AB, Vaughan ED, Wein AJ, editors. Campbell's urology. 7th edn. Vol. 3. Philadelphia: WB Saunders; 1998;2853–2863.
2. Jordan GH, Schlossberg SM, Devine CJ. Surgery of the penis and urethra. In: Walsh PC, Retik AB, Vaughan ED, Wein AJ, editors. Campbell's urology. 7th edn. Vol. 3. Philadelphia: WB Saunders; 1998;3341–3347.
3. Rosen MA, Nash PA, Bruce JE, McAninch JW. The actuarial success rate of surgical treatment of urethral strictures. J Urol 1994;151:360A (Abstract).
4. Albers P, Fichtner J, Bruhl P, Muller SC. Long-term results of internal urethrotomy. J Urol 1996;156:1611–1614.
5. Benchekroun A, Lachkar A, Soumana A, Farih MH, Belahnech Z, Marzouk M, Faik M. Internal urethrotomy in the treatment of urethral stenoses (longterm results). Ann Urol (Paris) 1998;32:99–102.
6. Heyns CF, Steenkamp JW, De Kock ML, Whitaker P. Treatment of male urethral strictures: Is repeated dilation or internal urethrotomy useful? J Urol 1998;160:356–358.

7. Klammert R, Schneede P, Kriegmair M. Die laserbehandlung von Harnrohrenstrikturen. Urologie A 1994;33:295–298.
8. McNicholas TA, Colles J, Bown SG, Wickham JEA. Treatment of urethral strictures with a prototype CO_2 laser endoscope. Lasers Med Sci 1988;3:427.
9. Adkins WC. Argon laser treatment of urethral stricture and vesical neck contracture. Lasers Surg Med 1988;8:600–603.
10. Becker H Ch, Miller J, Noske HD, Klask JP, Weidner W. Transurethral laser urethrotomy with argon laser: Experience with 900 urethrotomies in 450 patients from 1978–1993. Urol Int 1995;55:150–153.
11. Shanberg A, Baghdassarian R, Tansey L, Sawyer D. K.T.P. 532 laser in treatment of urethral strictures. Urology 1988; 32:517–520.
12. Turek PJ, Malloy TR, Cendron M, Carpiniello VL, Wein AJ. KTP-532 laser ablation of urethral strictures. Urology 1992; 40:330–334.
13. Smith JA, Dixon JA. Neodymium:YAG laser treatment of benign urethral strictures. J Urol 1984;131:1080–1081.
14. Smith JA. Treatment of benign urethral strictures using a sapphire tipped neodymium:YAG laser. J Urol 1989;142: 1221–1222.
15. Dogra PN, Nabi G. Core-through urethrotomy using the neodymium:YAG laser for obliterative urethral strictures after traumatic urethral disruption and/or distraction defects: Long-term outcome. J Urol 2002;167:543–546.
16. Nabi G, Dogra PN. Endoscopic management of post-traumatic prostatic and supraprostatic strictures using Neodymium-YAG laser. Int J Urol 2002;9(12):710–714.
17. Singal RK, Denstedt JD, Razvi HA, Chun SS. Holmium:YAG laser endoureterotomy for treatment of ureteral stricture. Urology 1997;50:875–880.
18. Gerber GS, Kuznetzov D, Leef JA, Rosenblum J, Steinberg GD. Ho:YAG laser endoureterotomy in the treatment of ureteroenteric strictures following orthotopic urinary diversion. Tech Urol 1999;5:45–48.
19. Hibi H, Mitsui K, Taki T, Mizumoto H, Yamamda Y, Honda N, Fukatsu H. Holmium laser incision technique for ureteral stricture using a small-calibre ureteroscope. JSLS 2000;4: 214–220.
20. Kural AR, Coskuner ER, Cevik I. Holmium laser ablation of recurrent strictures of urethra and bladder neck: preliminary results. J Endourol 2000;14:301–304.
21. Laven BA, O'Connor RC, Steinberg GD, Gerber GS. Long-term results of antegrade endoureterotomy using the holmium laser in patients with ureterointestinal strictures. Urology 2001;58:924–929.
22. Kourambas J, Delvecchio FC, Preminger GM. Low-power holmium laser for the management of urinary tract calculi, strictures, and tumors. J Endourol 2001;15(5):529–532.
23. Matsuoka K, Inoue M, Iida S, Tomiyasu K, Noda S. Endoscopic antegrade laser incision in the treatment of urethral stricture. Urology 2002;60(6):968–972.
24. Watterson JD, Sofer M, Wollin TA, Nott L, Denstedt JD. Holmium:YAG laser endoureterotomy for ureterointestinal strictures. J Urol 2002;167(4):1692–1695.
25. Baur H, Schneider W, Altwein JE. Treatment of recurrent urethral strictures by photoablation with the EXCIMER laser. BAUS 1992;118 (Abstract).
26. Anidjar M, Mongiat-Artus P, Broulard JP, Meria P, Teillac P, Le Duc A, Berthon P, Cussenot O. Thermal radiofrequency induced porcine ureteral stricture: A convenient endourologic model. J Urol 1999;161:298–303.
27. Meria P, Anidjar M, Brouland JP, Teillac P, Le Duc A, Berthon P, Cussenot O. An experimental model of bulbar urethral stricture in rabbits using endoscopic radiofrequency coagulation. Urology 1999;53:1054–1057.
28. Teichman JMH, Chan KF, Cecconi PP, Corbin NS, Kamerer AD, Glickman RD, Welch AJ. Er:YAG versus Ho:YAG lithotripsy. J Urol 2001;165:876–879.
29. Chan KF, Lee H, Teichman JHM, Kamerer AD, McGuff HS, Vargas G, Welch AJ. Erbium:YAG laser lithotripsy mechanism. J Urol 2002;168(2):436–441.
30. Fried NM. Potential applications of the Erbium:YAG laser in endourology. J Endurol 2001;15(9):889–894.
31. Fried NM, Long GM. Erbium:YAG laser ablation of urethral and ureteral tissues. Proc SPIE: Lasers Urol 2002;4609:122–127.
32. Walsh JT, Deutsch TF. Er:YAG laser ablation of tissue: Measurement of ablation rates. Lasers Surg Med 1989;9: 327–337.
33. Walsh JT. 1988. Pulsed ablation of tissue: Analysis of the removal process and tissue healing. Ph.D. Thesis. Northwestern University, Evanston, IL.
34. Wesendahl T, Janknecht P, Ott B, Frenz M. Erbium:YAG laser ablation of retinal tissue under perfluorodecaline: Determination of laser-tissue interaction in pig eyes. Invest Ophthalmol Vis Sci 2000;41:505–512.
35. Walsh JT, Flotte TJ, Deutsch TF. Er:YAG laser ablation of tissue: Effect of pulse duration and tissue type on thermal damage. Lasers Surg Med 1989;9:314–326.
36. Hill RA, Stern D, Lesiecki ML, Hsia J, Berns MW. Effects of pulse width on erbium:YAG laser photothermal trabecular ablation (LTA). Lasers Surg Med 1993;13:440–446.
37. Sporri S, Frenz M, Altermatt HJ, Bratschi HU, Romano V, Forrer M, Dreher E, Weber HP. Effects of various laser types and beam transmission methods on female organ tissue in the pig: An in vitro study. Lasers Surg Med 1994;14:269–277.
38. Brazitkos PD, D'Amico DJ, Bochow TW, Hmelar M, Marcellino GR, Stangos NT. Experimental ocular surgery with a high-repetition-rate erbium:YAG laser. Invest Ophthalmol Vis Sci 1998;39:1667–1675.

Lasers in Surgery and Medicine 34:5–11 (2004)

Hybrid Germanium/Silica Optical Fibers for Endoscopic Delivery of Erbium:YAG Laser Radiation

Charles A. Chaney, MS, Yubing Yang, PhD, and Nathaniel M. Fried, PhD*
Biophotonics Laboratory, Department of Urology, Johns Hopkins Medical School, Baltimore, Maryland 21224

Background and Objectives: Endoscopic applications of the erbium (Er):YAG laser have been limited due to the lack of an optical fiber delivery system that is robust, flexible, and biocompatible. This study reports the testing of a hybrid germanium/silica fiber capable of delivering Er:YAG laser radiation through a flexible endoscope.
Study Design/Materials and Methods: Hybrid optical fibers were assembled from 1-cm length, 550-μm core, silica fiber tips attached to either 350- or 425-μm germanium oxide "trunk" fibers. Er:YAG laser radiation ($\lambda = 2.94$ μm) with laser pulse lengths of 70 and 220 microseconds, pulse repetition rates of 3–10 Hz, and laser output energies of up to 300 mJ was delivered through the fibers for testing.
Results: Maximum fiber output energies measured 180 ± 30 and 82 ± 20 mJ ($n = 10$) under straight and tight bending configurations, respectively, before fiber interface damage occurred. By comparison, the damage threshold for the germanium fibers without silica tips during contact soft tissue ablation was only 9 mJ ($n = 3$). Studies using the hybrid fibers for lithotripsy also resulted in fiber damage thresholds (55–114 mJ) above the stone ablation threshold (15–23 mJ).
Conclusions: Hybrid germanium/silica fibers represent a robust, flexible, and biocompatible method of delivering Er:YAG laser radiation during contact soft tissue ablation. However, significant improvement in the hybrid fibers will be necessary before they can be used for efficient Er:YAG laser lithotripsy. Lasers Surg. Med. 34:5–11, 2004.

Key words: erbium; laser; lithotripsy; stricture; ureter; urethra; germanium; sapphire; fiber

INTRODUCTION

The erbium (Er):YAG laser has been used extensively for precision ablation of tissue in medical fields which do not require a flexible optical fiber delivery system, such as dermatology [1,2], dentistry [3,4], and ophthalmology [5–11]. In these fields, the use of an articulated arm delivery system or semi-rigid optical fibers, although not ideal, are adequate for performing surgery. However, for medical applications requiring delivery of laser radiation through a flexible endoscope (e.g., the upper urinary tract), current laser delivery systems for the Er:YAG laser remain inadequate.

Although there are several types of optical fibers and waveguides available for delivery of mid-infrared laser radiation, including chalcogenide, zirconium fluoride, sapphire, germanium oxide, and hollow silica waveguides, all of these delivery systems have major limitations [12–14]. The chalcogenide fibers cannot handle high power, they are toxic, and they break easily. The zirconium fluoride fibers are also brittle, hygroscopic, and toxic in tissue. The sapphire fibers must be polished as well as cleaved, and suffer from mechanical stress and breakage during tight bending conditions. The germanium oxide fiber tips damage at low output energies during contact tissue ablation due to their low melting temperature. The hollow silica waveguides are not biocompatible and are limited in their bending ability with high transmission losses during tight bending. Thus, the ideal mid-infrared optical fiber that combines high-power delivery, flexibility, chemical and mechanical durability, and biocompatibility, has yet to be successfully tested.

The goal of this study is to test a hybrid optical fiber with the Er:YAG laser, which combines the high-power transmission and flexibility of the germanium oxide fiber with the robust and biocompatible low-OH silica fiber tips currently in clinical use with the holmium (Ho):YAG laser. Although increased absorption limits the use of long low-OH silica fibers beyond wavelengths of approximately 2.5 μm, previous studies have demonstrated that short low-OH silica fiber lengths, on the order of a few centimeters, are capable of transmitting sufficient Er:YAG laser energy for soft tissue ablation [5,6,8,15]. We demonstrate in this study that long hybrid fibers are capable of being assembled with a simple process that reduces many of the limitations associated with current mid-IR optical fibers, and that sufficient Er:YAG laser energy can be

Contract grant sponsor: NIH Phase I SBIR grant awarded to Infrared Fiber Systems (Silver Spring, MD); Contract grant number: 1R43 EY13889-01; Contract grant sponsor: National Kidney Foundation of Maryland (Professional Development Award); Contract grant sponsor: Department of Defense Prostate Cancer Research Program (New Investigator Award); Contract grant number: DAMD17-03-0087; Contract grant sponsor: A. Ward Ford Memorial Institute (American Society for Laser Medicine and Surgery).
*Correspondence to: Nathaniel M. Fried, PhD, Department of Urology, Johns Hopkins Bayview Medical Center, 4940 Eastern Avenue, Building A, Room 347c, Baltimore, MD 21224.
E-mail: nfried@jhmi.edu
Accepted 13 October 2003
Published online in Wiley InterScience (www.interscience.wiley.com).
DOI 10.1002/lsm.10249

transmitted through these fibers during insertion into a flexible endoscope for potential use in multiple soft and hard tissue laser ablation applications.

MATERIALS AND METHODS

Laser Parameters

An Er:YAG laser (SEO 1-2-3, Schwartz Electro-Optics, Orlando, FL) operating at a wavelength of 2.94 μm was connected to either a fixed long-pulse laser power supply (220-microseconds pulse length, 400 mJ/pulse) or a variable pulse width laser power supply (Model 8800V, Analog Modules, Longwood, FL), producing up to 30 mJ per pulse at 70-microseconds pulse-lengths. The laser radiation was externally focused with a 50-mm focal-length calcium fluoride lens into either 250, 350, or 425-μm core germanium oxide optical fibers (Infrared Fiber Systems, Silver Spring, MD), with and without silica fiber tips attached to the output end of the germanium "trunk" fiber. Fiber output energy was measured using a pyroelectric detector (Gentec ED-200, Ste.-Foy, Que.), and the laser pulse duration was measured using a photovoltaic infrared detector (PD-10.6, Boston Electronics, Brookline, MA).

Germanium "Trunk" Fibers

Preliminary laser ablation tests were conducted with 250-μm core and 425-μm core germanium oxide fibers in direct contact with ex vivo samples of soft urological tissues, including canine prostatic urethral tissue and porcine ureteral tissue. A total of 500 pulses were delivered with a pulse length of 70 microseconds and a pulse repetition rate of 10 Hz. Pre- and post-ablation fiber output energies were measured to determine whether any damage occurred to the fiber tip. A decay in fiber output greater than 5% of the initial energy was considered significant. An optical microscope was also used to analyze the output ends of the germanium fibers for evidence of fiber tip degradation after contact tissue ablation in an effort to gain insight into the mechanism of fiber damage.

Hybrid Fiber Assembly

The hybrid fiber consisted of a 1-cm long, 550-μm core, low-OH silica fiber tip attached to either a 350-μm core or 425-μm core germanium oxide trunk fiber using several different methods. For all of these methods, the initial fiber preparation was similar. The germanium fiber jacket was softened using chemical treatment (1-methyl-2-pyrrolidinone at 150°C for 2 minutes then isopropanol for 3 minutes) and then stripped with a razor blade. Both the germanium and silica fiber tips were polished with rough 600-grit and then fine 5-micron sandpaper. The fibers were then aligned under a stereoscopic microscope for attachment using a laboratory-constructed mechanical setup consisting of optical fiber chucks, positioners, and linear and rotational stages.

Several different methods of attachment were explored (Fig. 1). First, index-matching UV-cured optical epoxy (Norland, New Brunswick, NJ) was applied with a syringe needle either around the fibers or at the fiber interface

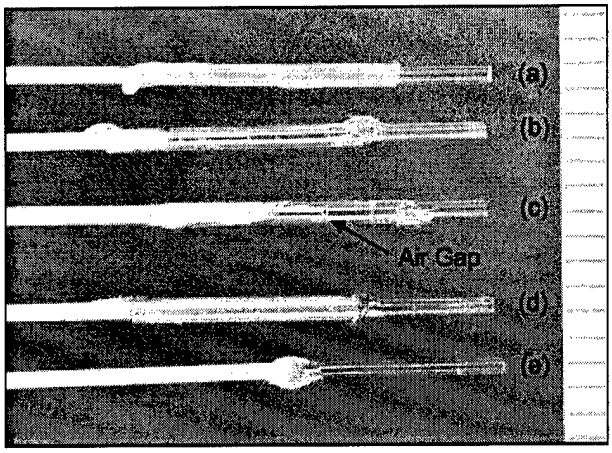

Fig. 1. Image of the germanium/silica hybrid fibers assembled using five different methods: (**a**) heat-shrink tubing, (**b**) glass capillary tubing, (**c**) glass tubing with an air gap at the fiber interface, (**d**) stainless steel hypodermic tubing, and (**e**) UV-cured optical epoxy. For all of the methods, an approximately 1-cm long, 550-μm core, low-OH silica tip was attached to a 425-μm core germanium trunk fiber. Ball-shaped glue drops are present in (b–e) at the interface between the yellow germanium jacket and the conduit material and at the interface between the silica tip and the conduit. The ruler lines = 1 mm.

(n = 10 fibers). Second, 30-G PTFE heat shrink tubing (normal ID = 850 μm, shrunk ID = 375 μm, wall thickness = 150 μm, length = 5 mm) was shrunk around the germanium/silica fiber interface using a heat gun (n = 10 fibers). The PTFE tubing (Small Parts, Inc., Miami Lakes, FL) also served the purpose of acting as a biocompatible jacket surrounding any exposed germanium fiber. Third, stainless steel hypodermic tubing (Small Parts, Inc., ID = 0.675 mm, OD = 1.05 mm) was used to align the fibers (n = 5 fibers). Fourth, glass capillary tubing (VitroCom, Mountain Lakes, NJ, ID = 0.7 mm, OD = 0.87 mm) was used as a conduit for fiber attachment. For the glass tubing, two methods of attachment were explored: with the fibers in contact at the interface (n = 10 fibers) and with a small air gap (~200 μm) at the fiber interface (n = 10 fibers).

Fiber Transmission and Bending Tests

Preliminary fiber bending tests were conducted with germanium and sapphire optical fibers, ranging in core diameter from 150 to 500 μm. The fibers were inserted into a 15 Fr (5 mm) flexible cysto-urethroscope with a 7 Fr (2.3 mm) working channel. After insertion, basic fiber testing was performed to determine whether the fiber could withstand high-mechanical stress under tight bending conditions and whether the fiber presence hindered maximum deflection of the scope. Peak energy transmission of the Er:YAG laser radiation through the hybrid fibers was then measured for both straight and bent configurations

(with the fibers bent just above their minimum breaking radius of 15 mm for the 350 μm fiber and 25 μm for the 425 μm fiber).

Stone Ablation Studies

Limited studies were also performed with the Er:YAG laser and the hybrid (350/550 and 425/550) fibers for contact tissue ablation of urological stones. The goal of these studies was to demonstrate that sufficient energy could be delivered through the hybrid fibers in contact mode for endoscopic ablation of the stones. Human uric acid and calcium oxalate monohydrate (COM) stones were obtained from a stone analysis laboratory (UroCore LabCorp, Oklahoma City, OK), sectioned with a water-cooled band saw into cylindrical samples (diameter = 8–10 mm), and then weighed with an analytical balance (dry weight = 300–450 mg). The stone samples were then placed in a water bath, and the hybrid fiber tip placed in contact with the stone. Er:YAG laser radiation was delivered to the stone with pulse lengths of 220 microseconds, pulse repetition rates of 3 Hz, and fiber output energies of from 5 to 150 mJ.

Data Analysis

For the fiber damage studies, a total of 500 laser pulses was delivered through the fiber at each energy level between pre- and post-testing measurements. For the bare germanium fibers, the measurements were done during contact soft tissue ablation and represented the fiber tip damage threshold. For the hybrid fiber testing, measurements were initially made in air and then in contact with the stone samples. Maximum fiber output energy was recorded as the mean ± standard deviation (SD) for N samples tested.

Statistical analysis was conducted between the data sets for maximum pulse energies achieved with each method of hybrid fiber assembly. Analysis of variance (ANOVA) was used to determine statistical significance between data sets. A value of $P < 0.05$ was considered to be statistically significant.

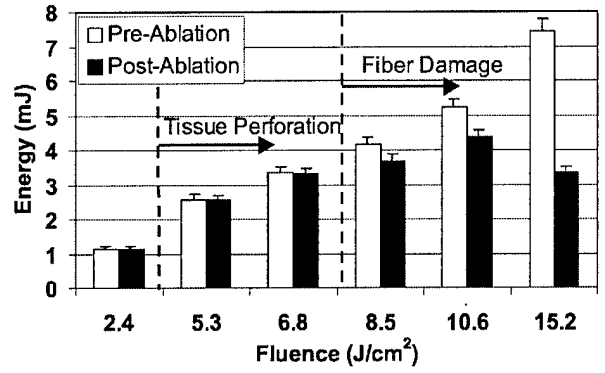

(a) 250-μm-core Germanium Fiber

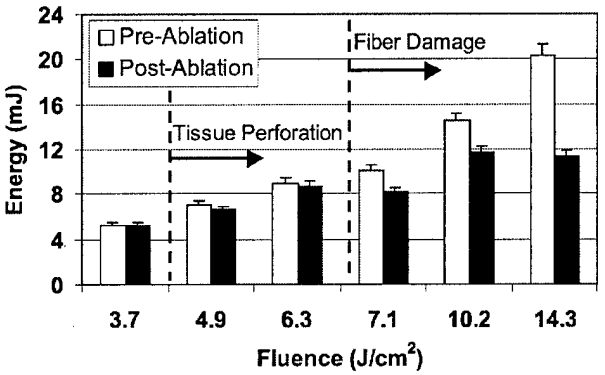

(b) 425-μm-core Germanium Fiber

Fig. 2. Germanium oxide fiber damage thresholds for (**a**) 250-μm core fibers, and (**b**) 425-μm core fibers. A total of 500 pulses were delivered with a pulse length of 70 microseconds and a pulse repetition rate of 10 Hz. The fiber tip was in direct contact with the tissue. Error bars signify a ±5% variation in pulse to pulse energy stability.

RESULTS

Germanium Trunk Fibers

Preliminary laser ablation tests were conducted with 250-μm core and 425-μm core germanium oxide fibers in direct contact with ex vivo samples of soft urological tissues. For laser pulse lengths of 70 microseconds, the fiber damage thresholds were 4 mJ (7 J/cm^2) and 9 mJ (6 J/cm^2) for the 250-μm and 425-μm fibers, respectively (Fig. 2). These values are above the threshold for perforating samples of ureteral tissue, 2 mJ (4.1 J/cm^2) and 5.1 mJ (3.7 J/cm^2), respectively [16]. However, the germanium oxide fiber by itself is nevertheless limited to operation at relatively low laser energies during contact tissue ablation due to the potential for fiber tip damage.

The primary mechanism of germanium fiber damage during contact soft tissue ablation is melting of the fiber tip due to the high ablative temperatures. Figure 3 shows the fiber tips at different stages of meltdown, as described by the transition from the normal tip surface to particle formation, cracking and charring of the fiber tip, and finally catastrophic meltdown and failure as evidenced by crystalline formation. During these progressive phases of fiber degradation, the fiber output energy also steadily dropped.

It should be noted, however, that there was no evidence of fiber damage when the germanium fibers were used previously for tissue ablation in non-contact mode. These trunk fibers have successfully transmitted up to 20 W of power (2 J at 10 Hz) without problem [17].

Hybrid Germanium/Silica Fibers

To overcome the limitations of the germanium fiber for contact tissue ablation, a hybrid fiber consisting of a short low-OH silica fiber tip was attached to the germanium trunk fiber using several different methods, including: (a) UV-cured optical epoxy, (b) stainless steel hypodermic tubing, (c) capillary glass tubing, and (d) heat-shrink tubing. Table 1 shows the average output energy transmitted through the fiber for each of these methods before a

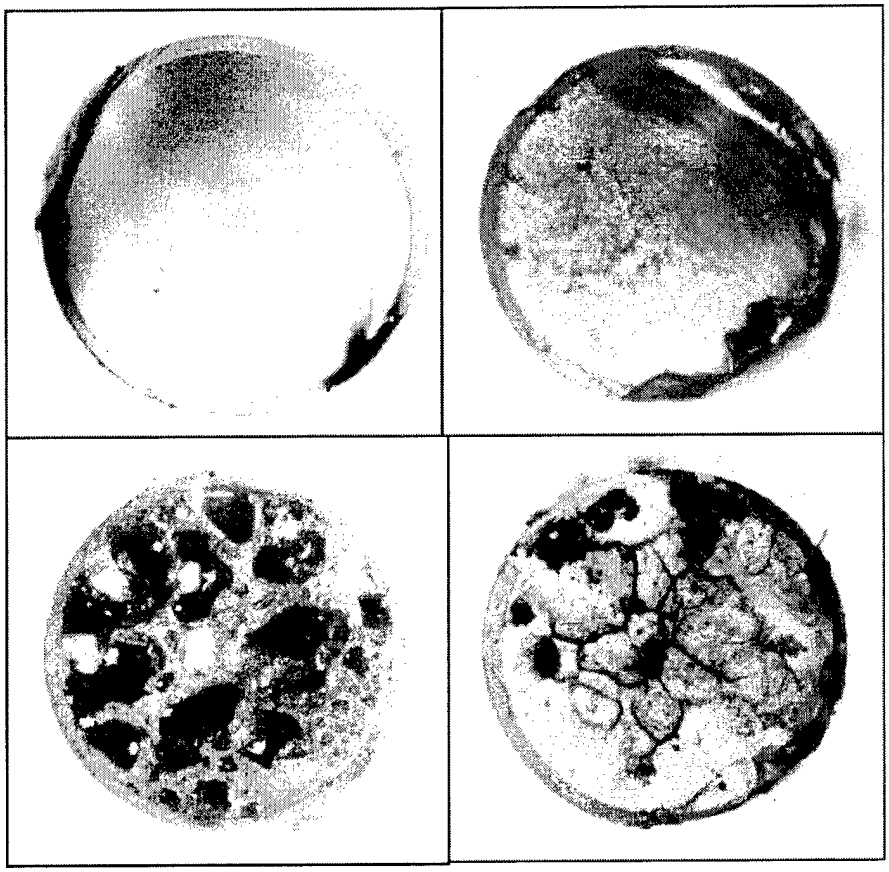

Fig. 3. Mechanism of germanium oxide fiber tip damage when tested in contact with tissue. Clockwise images starting from top left show (**a**) normal fiber tip, (**b**) particulate formation on the fiber tip, (**c**) cracking and charring, and (**d**) crystalline formation. The progressive deterioration is due to melting of the fiber tip when in contact with the tissue during high-temperature tissue ablation. Fiber tip damage was not observed during non-contact ablation studies. The parameters were: 425-μm core fiber, 10 mJ/pulse, 70-microseconds pulse duration, 10 Hz pulse repetition rate, and a total of 500 pulses. [Figure can be viewed in color online via www.interscience.wiley.com].

drop in output energy was observed due to damage at the germanium/silica interface. The damage threshold for the germanium fiber without silica tip during contact soft tissue ablation is also included for comparison. Using the heat-shrink tubing method, hybrid fiber output energies measured 180 ± 30 mJ (76 ± 13 J/cm^2), before fiber damage was observed ($n = 10$). This was significantly higher than that achieved with germanium fiber and silica tips attached with any of the other methods ($P \leq 0.05$). Although the results of the glass capillary tubing were more promising, there was no statistical difference between glass fiber assembly with or without a small air gap at the germanium/silica interface ($P = 0.10$).

Fiber Bending and Transmission Tests

Earlier tests showed that the sapphire optical fibers were more robust than the germanium fibers, as evidenced by the difference in their melting temperatures (2,030 vs. 680°C) and the absence of fiber tip damage during contact soft tissue ablation [12,18]. However, the sapphire fiber was not pursued further because both 250- and 425-μm core sapphire fibers suffered multiple fractures upon insertion into the flexible cysto-urethroscope under tight bending conditions (Table 2). While the 425-μm core germanium fibers also fractured upon repeated bending, the 150-, 250-, and 350-μm core germanium fibers suffered no mechanical damage under similar test conditions. Figure 3 shows a 350-μm core germanium oxide fiber inserted through the 7 Fr working channel of a 15 Fr flexible cysto-urethroscope. The scope was deflected at a maximum angle corresponding to a bend radius of approximately 15 mm with and without the fiber inserted (Fig. 4).

Both the 350/550 and 425/550 germanium/silica hybrid fibers showed a significant decrease in energy output when bent to just above their minimum bending radius, 15 mm for the 350 μm trunk fiber and 25 mm for the 425 μm trunk fiber (Table 3). The damage mechanism was usually observed as sparking at the germanium/silica fiber interface, resulting in a melting of the germanium surface at the fiber interface, and noted as an immediate loss in energy greater than 5%. The difference in results between the 350- and 425-μm trunk fibers can be explained in part by the

TABLE 1. Comparison of Results for Different Materials and Methods Used to Construct Germanium/Silica Hybrid Fibers

Assembly method[a]	Maximum pulse energy (mJ)	N
Germanium tip only[b]	9 ± 1	3
Silica tip attached with		
UV-cured epoxy	10 ± 5	10
Steel hypodermic tubing	109 ± 47	10
Glass capillary tubing		
With air gap at interface	104 ± 38	10
Without air gap at interface	139 ± 49	10
Heat-shrink tubing	180 ± 30	10

[a]All fibers were constructed using a 425-μm core germanium trunk fiber and a 1-cm long, 550-μm core silica fiber tip. The fibers were tested using an erbium (Er):YAG laser with a 220 microseconds laser pulse length at 3 Hz.

[b]Values for the germanium fibers without silica tip represent maximum pulse energies achieved during contact soft tissue ablation. No problems were encountered during non-contact ablation.

difference in the cross-sectional area at the germanium fiber tip. Assuming the melting temperature of the germanium fiber tip at the interface is the limiting factor, the maximum fluence that the interface can handle before melting is a function of both energy and fiber diameter. Thus, a larger trunk fiber diameter transmits greater energy, as observed in Table 3.

Lithotripsy Studies

Both the 350/550 and 425/550 hybrid germanium/silica fibers were tested for Er:YAG laser ablation of uric acid and COM stones. The ablation threshold for the stones and the peak energies transmitted through the fibers before fiber interface damage occurred was measured (Table 4). Ablation craters were first observed in the stones at energy levels of 15–23 mJ. There was no statistically significant dependence on stone type or trunk fiber used. The peak energies, however, were again dependent on fiber trunk diameter (350 or 425 μm), similar to the previous results for the fiber bending studies.

TABLE 2. Preliminary Bending Tests Performed Using a 15 Fr Flexible Cysto-Urethroscope With a 7 Fr Working Channel and a Bend Radius of ~15 mm

Fiber type/core size	Minimum bend radius[a]	Flexible scope breaking test
Sapphire		
150 μm	20 mm	Passed
250 μm	30 mm	Failed
325 μm	60 mm	Not tested
425 μm	80 mm	Failed
Germanium oxide		
150 μm	5 mm	Passed
250 μm	10 mm	Passed
350 μm	15 mm	Passed
425 μm	25 mm	Failed
500 μm	40 mm	Failed

[a]Values for the minimum bend radius are taken from commercial literature (www.photran.com and www.infrared-fibersystems.com).

DISCUSSION

Several applications in urology may benefit from the availability of a suitable optical fiber delivery system for tissue ablation using the erbium:YAG laser. Potential applications include more precise laser incision of ureteral and urethral strictures and more efficient laser lithotripsy. Previous studies by our research group suggest that Er:YAG laser incision of the ureter and urethra reduces peripheral thermal damage by a factor of 10 in comparison with the Ho:YAG laser (30 ± 10 vs. 290 ± 30 μm), which may translate into less scarring and improved success rates during clinical application [14,16,18].

Teichmann et al. have reported that Er:YAG laser lithotripsy is approximately 2.4 times more efficient than Ho:YAG laser lithotripsy (53.6 ± 38.7 vs. 22.6 ± 6.4 gμm/J), and that the lack of a reliable optical fiber delivery system is the major limitation to clinical application of Er:YAG laser lithotripsy [19]. They demonstrated that both the 425-μm core sapphire and germanium fibers suffered significant degradation during Er:YAG laser lithotripsy studies, with fiber output energies declining to less than 70% of their initial 100 and 200 mJ energies, respectively [20]. Other experiments with the sapphire fiber were limited to energies of 50 mJ (35 J/cm^2) to minimize fiber damage [21].

Recently, Papagiakoumou et al. have also reported the characterization of the germanium oxide fibers for flexible transmission of Er:YAG laser radiation [22]. They reported that the fibers exhibited no significant bending losses when bent to a radius of 40 mm and transmitting up to 20 mJ of energy. While these testing conditions were different than those of the current study (e.g., no silica tip, lower energy transmission, and higher bend radius), they nevertheless further demonstrated the potential of the germanium fiber as a flexible delivery system.

When comparing our methods used to assemble the hybrid fibers, it should be noted that there was a large difference in peak output energy between some of the methods. The bare germanium fibers and hybrid fibers attached with epoxy performed poorly in comparison with the hybrid fibers attached with metal, glass, and heat-shrink tubing. This can be explained again by considering the low-melting temperature of the germanium fiber. The epoxy presumably acted as an absorbing material, resulting in thermal buildup at the interface, and eventual fiber decay and transmission loss. On the contrary, the heat-shrink and glass tubing were more efficient in transmitting coupling losses at the fiber interface through the wall, resulting in less thermal buildup. Also, it should be noted that alignment of the germanium/silica fiber interface inside the steel tubing was difficult because the material

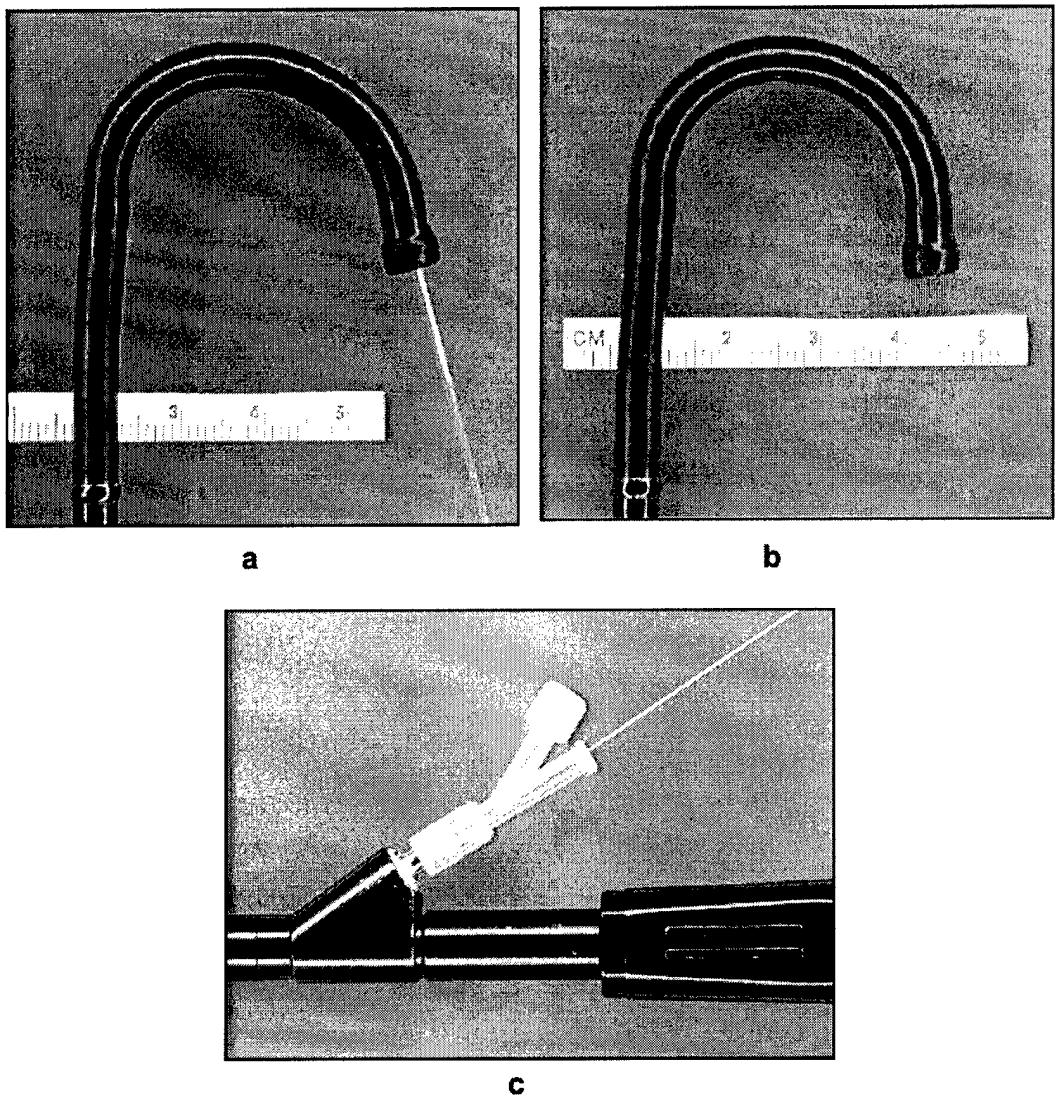

Fig. 4. Images of a 350-μm core germanium/silica hybrid fiber inserted through a 15 Fr flexible cysto-urethroscope with a 7 Fr working channel. **a**: The fiber is bent to a radius of approximately 15 mm without breaking under maximum scope deflection. **b**: Maximum deflection of the scope without fiber present also corresponds to a radius of approximately 15 mm, demonstrating that the fiber does not significantly hinder scope deflection. **c**: The fiber is successfully inserted at a 30° angle into the working channel.

was not transparent, unlike the other materials used for assembly (glass, heat-shrink tubing).

The performance of the hybrid fibers was also limited when the fibers were placed either in tight bending configurations or in contact with hard tissue (e.g., stones). Some of the fiber damage and transmission losses may be due to limitations in the spatial and temporal beam quality of the input laser beam and the introduction of higher modes during bending. Future research will focus on delivering a single mode Gaussian or flat-top spatial beam profile and eliminating the micro-pulse spikes that compose the Er:YAG temporal beam profile [16].

TABLE 3. Damage Thresholds During Germanium/ Silica Fiber Bending Tests

Fiber core (μm) (trunk/tip)	Peak energy (mJ)		Bend radius (mm)	N
	Straight	Bent		
425/550	180 ± 30	82 ± 20	30	10
350/550	93 ± 13	65 ± 20	20	10

Overall, however, our results show that by adding a robust silica fiber tip to the germanium fiber, fiber output energies may be increased to 180 ± 30 mJ (76 ± 13 J/cm^2) and 82 ± 20 mJ (35 ± 9 J/cm^2), in straight and tight bending configurations, respectively, without fiber damage. This represents a large improvement over the 9 mJ (6 J/cm^2)

TABLE 4. Results Using Hybrid Germanium/Silica Fibers for Er:YAG Lithotripsy

Fiber core (μm) (trunk/tip)	Stone type	Stone ablation threshold (mJ)	Fiber damage threshold (mJ)	N
350/550	Uric acid	15 ± 2	55 ± 8	3
	COM	22 ± 5	63 ± 11	3
425/550	Uric acid	19 ± 1	90 ± 32	4
	COM	23 ± 9	114 ± 8	4

COM, calcium oxalate monohydrate.

peak energy achieved during testing of the bare germanium fiber in contact with soft tissue (Fig. 1b). While these results demonstrate that the hybrid germanium/silica fiber currently transmits sufficient energy for contact soft tissue ablation through a flexible endoscope, further improvements will be necessary before the hybrid fiber can be used effectively for Er:YAG laser lithotripsy. These fiber output energies are still too low to efficiently ablate stones at a rate suitable for clinical use. We are currently working to further refine our hybrid fiber assembly method to provide even higher and more consistent Er:YAG laser output energy and smaller, more flexible fibers for use in flexible endoscopes.

CONCLUSIONS

A robust, flexible, and biocompatible hybrid germanium/silica fiber was assembled capable of delivering Er:YAG laser radiation through a flexible endoscope. This fiber may serve as a reliable delivery system with the Er:YAG laser for applications in the urological tract, which may benefit from more precise and efficient laser ablation. Such applications may include laser incision of urethral and ureteral strictures and laser lithotripsy. Assembly of smaller diameter hybrid fibers, more rigorous endoscope bending tests, and achievement of higher fiber output energy thresholds will all be pursued in the further development and testing of these hybrid fibers.

ACKNOWLEDGMENTS

We thank Ken Levin, Dan Tranh, and Alex Tchap of Infrared Fiber Systems, for providing the germanium oxide optical fibers used in these experiments.

REFERENCES

1. Kaufmann R. Role of the erbium:YAG laser in the treatment of aged skin. Clin Exp Dermatol 2001;26(7):631–636. (Review).
2. Alster TS, Lupton JR. Erbium:YAG cutaneous laser resurfacing. Dermatol Clin 2001;19(3):453–466. (Review).
3. Rechmann P, Glodin DS, Hennig T. Er:YAG lasers in dentistry: An overview. Proc SPIE: Lasers Dent IV 1998; 3248:2–13.
4. Clarkson DM. A review of technology and safety aspects of erbium lasers in dentistry. Dent Update 2001;28(6):298–302.
5. Ozler SA, Hill RA, Andrews JJ, Baerveldt G, Berns MW. Infrared laser sclerostomies. Invest Ophthalmol Vis Sci 1991;32(9):2498–2503.
6. Hill RA, Baerveldt G, Ozler SA, Pickford M, Profeta GA, Berns MW. Laser trabecular ablation (LTA). Lasers Surg Med 1991;11(4):341–346.
7. McHam ML, Eisenberg DL, Schuman JS, Wang N. Erbium:YAG laser trabecular ablation with a sapphire optical fiber. Exp Eye Res 1997;65:151–155.
8. Stevens G, Jr., Long B, Hamann JM, Allen RC. Erbium:YAG laser-assisted cataract surgery. Ophthalmic Surg Lasers 1998;29(3):185–189.
9. Brazitkos PD, D'Amico DJ, Bochow TW, Hmelar M, Marcellino GR, Stangos NT. Experimental ocular surgery with a high-repetition-rate erbium:YAG laser. Invest Ophthalmol Vis Sci 1998;39:1667–1675.
10. Neubaur CC, Stevens G, Jr. Erbium:YAG laser cataract removal: Role of fiber-optic delivery system. J Cataract Refract Surg 1999;25(4):514–520.
11. Wesendahl T, Janknecht P, Ott B, Frenz M. Erbium:YAG laser ablation of retinal tissue under perfluorodecaline: Determination of laser-tissue interaction in pig eyes. Invest Ophthalmol Vis Sci 2000;41:505–512.
12. Harrington JA. A review of infrared fibers. http://irfibers.rutgers.edu/ir-rev-index.html. Adapted from the OSA Handbook, Vol. III (Michael Bass, editor), McGraw-Hill, 2000.
13. Merberg GN. Current status of infrared fiber optics for medical laser power delivery. Lasers Surg Med 1993;13:572–576.
14. Fried NM. Potential applications of the erbium:YAG laser in endourology. J Endurol 2001;15(9):889–894.
15. Mrochen M, Riedel P, Donitsky C, Seiler T. Erbium:yttrium–aluminum–garnet laser induced vapor bubbles as a function of the quartz fiber tip geometry. J Biomed Opt 2001;6(3):344–350.
16. Fried NM, Tesfaye Z, Ong AM, Rha KH, Hejazi P. Optimization of the Erbium:YAG laser for precise incision of ureteral and urethral tissues: In vitro and in vivo results. Lasers Surg Med 2003;33:108–144.
17. Personal communication with Alex Tchap. Infrared Fiber Systems, Inc., Silver Spring, MD.
18. Fried NM, Long GM. Erbium:YAG laser ablation of urethral and ureteral tissues. Proc SPIE: Lasers Urol 2002;4609:122–127.
19. Teichman JMH, Chan KF, Cecconi PP, Corbin NS, Kamerer AD, Glickman RD, Welch AJ. Er:YAG versus Ho:YAG lithotripsy. J Urol 2001;165:876–879.
20. Lee H, Ryan TR, Lee A, Teichman JH, Welch AJ. Feasibility study of Er:YAG lithotripsy. Lasers Surg Med 2003; 15(Suppl):12.
21. Chan KF, Lee H, Teichman JMH, Kamerer A, McGuff HS, Vargas G, Welch AJ. Erbium:YAG laser lithotripsy mechanism. J Urol 2002;168:436–441.
22. Papagiakoumou E, Papadopoulos DN, Anastasopoulou N, Serafetinides AA. Comparative evaluation of HP oxide glass fibers for Q-switched and free-running Er:YAG laser beam propagation. Opt Comm 2003;220:151–160.

Proc. SPIE: Lasers in Urology
In Press.

APPENDIX 3

Variable Pulsewidth Erbium:YAG Laser Ablation of the Ureter and Urethra In Vitro and In Vivo: Optimization of the Laser Fluence, Pulse Duration, and Pulse Repetition Rate

Nathaniel M. Fried[a*], Zelalem Tesfaye[a], Albert M. Ong[a], Koon H. Rha[a], Pooya Hejazi[b]
[a]Dept. of Urology, Johns Hopkins Medical Institutions, Baltimore, MD 21224
[b]Dept. Electrical Engineering & Computer Science, Johns Hopkins Univ., Baltimore, MD 21218

ABSTRACT

Stricture recurrence frequently occurs due to mechanical or thermal insult during endourologic treatment of ureteral and urethral strictures. Optimization of the Er:YAG laser for precise incision of strictures was conducted using ureteral and urethral tissue samples, ex vivo, and a laparoscopic porcine ureteral model with exposed ureter, in vivo. Erbium:YAG laser radiation with a wavelength of 2.94 microns, pulse lengths of 8, 70, and 220 microseconds, output energies of 2-35 mJ, fluences of 1-25 J/cm^2, and pulse repetition rates of 5-30 Hz, was delivered through germanium oxide optical fibers in contact with the tissue. Incision of the ureteral wall was achieved in vivo with less than 20 pulses at a laser fluence of 4 J/cm^2. Thermal damage was reduced from 30-60 microns to 10-20 microns by shortening the laser pulse duration from 220 to 70 microseconds. Pulse repetition rates above 20 Hz resulted in larger thermal damage zones ranging from 60-120 microns. The Er:YAG laser, operating at a pulse duration of approximately 70 microseconds, a fluence of 4 J/cm^2 or greater, and a repetition rate less than 20 Hz, is capable of rapidly incising urethral and ureteral tissues, in vivo, with minimal thermal and mechanical side-effects.

Keywords: erbium, laser, stricture, urethra, ureter

1. INTRODUCTION

Urethral and ureteral strictures occur as a result of trauma caused during surgery (e.g. transurethral resection of the prostate, radical retropubic prostatectomy, minimally invasive prostate thermal therapies, and upper urinary tract endosurgery) [1,2]. Lumenal scarring and narrowing may then lead to incontinence and urinary tract infection.

Several minimally invasive techniques are available for treatment of urological strictures [1,2]. Balloon dilation and cold knife incision are the preferred methods of treatment, but they have widely variable success rates ranging from 20-80 % [3-6]. Balloon dilation is ineffective when there is scar tissue present, and may cause further stress-induced damage. Cold knife incision may also cause mechanical damage, resulting in stricture recurrence. Electrocautery and Ho:YAG laser produce significant thermal damage, which may induce further scar formation and re-stricture. None of these methods work well, and it is often necessary to repeatedly dilate or incise the stricture. However, multiple dilations or incisions of complicated strictures do not provide increased benefit, leaving patients without an effective method for treating recalcitrant scarring, voiding disfunction and urinary incontinence [2].

Several different lasers have been used for treating strictures [7], including CO_2 [8], argon [9,10], KTP [11,12], Nd:YAG [13-16], Ho:YAG [17-24], and excimer [25] lasers. Laser therapy has been sub-optimal due to stricture recurrence, caused by excessive thermal damage to adjacent tissue and subsequent scar formation. Recently, the Ho:YAG laser has been used for incision of strictures. However, the Ho:YAG laser produces 300-400 μm of peripheral thermal damage during soft tissue ablation, and therefore, may not be optimal for incision of strictures. Excessive thermal damage during stricture treatment may increase recurrence, as shown by animal models [26,27].

Previous studies have shown that the Er:YAG laser efficiently ablates soft tissues with minimal peripheral thermal damage. The Er:YAG laser is being used in several medical fields (e.g. dermatology, dentistry, and ophthalmology) which require precise tissue ablation. Recent applications of the Er:YAG laser in urology have also been reported, including lithotripsy [28,29], and incision of soft tissues for potential treatment of strictures [30,31]. The goal of this study is to optimize the Er:YAG laser parameters for rapid and precise incision of urethral and ureteral tissues.

*nfried@jhmi.edu; phone: 1 410 550 7906; fax: 1 410 550 3341

2. MATERIALS AND METHODS

2.1 Laser Parameters

An Erbium:YAG laser (SEO 1-2-3, Schwartz Electro-optics, Orlando, FL) operating at a wavelength of 2.94 μm was connected to a variable pulsewidth laser power supply (Model 8800V, Analog Modules, Longwood, FL), producing laser pulse lengths from 1-220 μs. The laser radiation was focused with a 50-mm-FL calcium fluoride lens into either 250-μm or 425-μm germanium oxide optical fibers (Infrared Fiber Systems, Silver Spring, MD). The laser was operated at pulse repetition rates of 5-30 Hz, pulse energies of 2-35 mJ, and fluences of 1-25 J/cm^2. The laser energy was measured using a pyroelectric detector (Gentec ED-200, Ste.-Foy, Quebec), and the pulse duration was measured using a photovoltaic infrared detector (PD-10.6, Boston Electronics, Brookline, MA). Figure 1 shows the temporal beam profiles from 1-220 μs. Ablation rate studies were performed at only the 8, 70, and 220 μs pulse lengths, because there was insufficient output energy for tissue ablation at the 1 μs pulse duration.

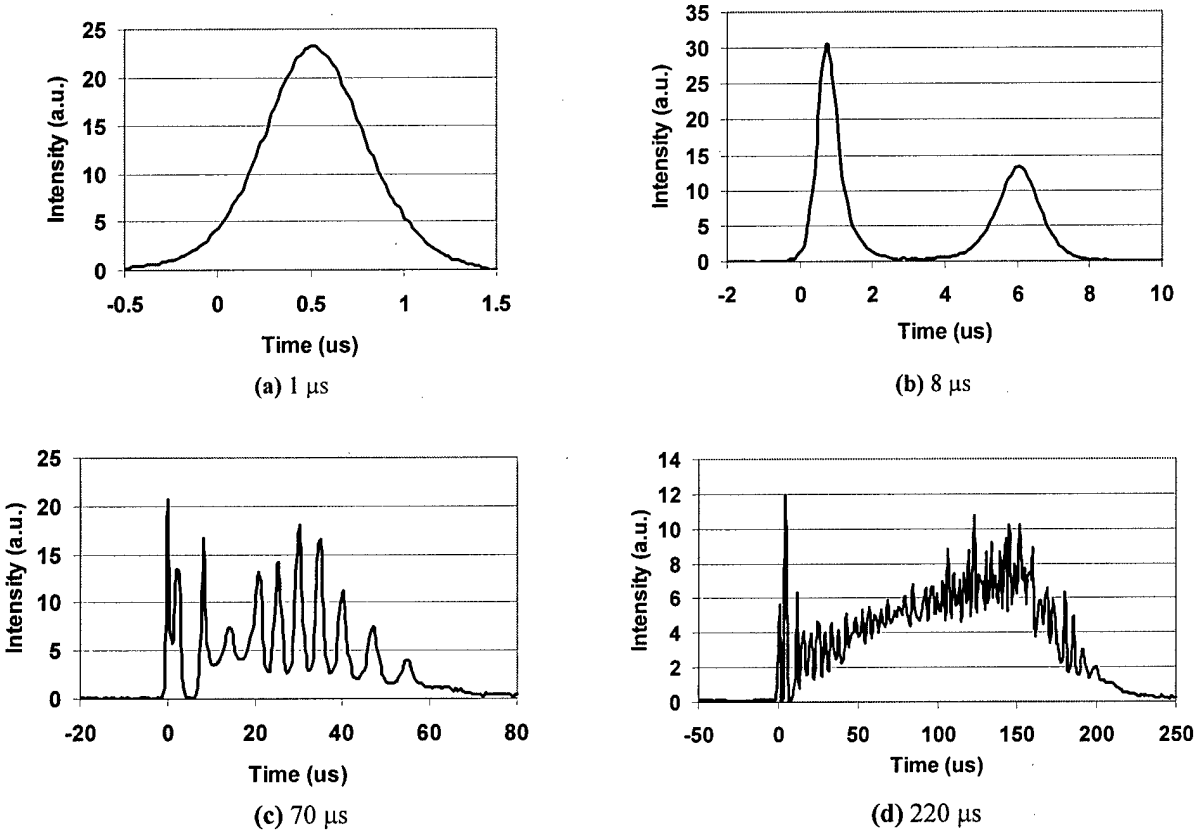

Figure 1. Temporal pulse profiles for the Er:YAG laser operated with laser pulse lengths of 1, 8, 70, and 220 μs.

2.2 In Vitro Tissue Preparation

Fresh ureteral tissue samples were removed from adult female pigs (100 kg) directly after sacrifice at the local slaughterhouse (Mt. Airy Locker Company, Mt. Airy, MD). Fatty tissue was shaved from the ureter with a scalpel blade, the tissue was spatulated, cut into 1 x 1 cm samples, stored in normal saline, and refrigerated for use within 24 hours. Fresh prostatic urethral tissue samples were obtained from male dogs (25-30 kg) after sacrifice for unrelated experiments at the Johns Hopkins Medical School. The posterior urethra was dissected from the prostate, spatulated, sectioned into 1 x 1 cm samples, stored in saline, and refrigerated.

For the ablation measurements, tissue samples were sandwiched between microscope and plexiglass slides to a fixed thickness (350 $\pm$ 50 μm), and the optical fiber tip positioned in contact with the sample through 2-mm-diameter holes drilled in the front plexiglass holder. The tissue samples were kept hydrated with saline using a syringe during the ablation experiments. The samples were placed in front of a pyroelectric detector, and the number of pulses required to perforate each sample was measured.

2.3 In Vivo Animal Experiments

All animal protocols were reviewed and approved by the Animal Care and Use Committee at the Johns Hopkins School of Medicine. A total of 4 female pigs (30-45 kg, Archer Farms, Belcamp, MD) were pretreated with acepromazine 0.39 mg/kg IM and ketamine 2 mg/kg IM. After the animals were sedated, intravenous access was obtained and normal saline administered as a 5 ml/cc bolus followed by a maintenance rate of 1.5 ml/kg/h. Intravenous propofol was administered for anesthesia. After adequate depth of anesthesia, the animal was positioned and laparoscopic ports were placed in the standard 3-port configuration, using a Visiport (US Surgical Corp., Norwalk, CT) for initial access. Using laparoscopic instrumentation, the ipsilateral ureter was identified and isolated, taking care to avoid excessive dissection and skeletonization. The distal ureter was ligated and transected close to the bladder. A small incision was made in the body wall and the ureter brought external to the body. The ureter was then spatulated and marked with 6-0 prolene sutures. The laser fiber was placed on the ureteral lumen, and the number of laser pulses required to perforate the ureter was recorded. An average of 12 perforations were made in each ureter, spaced approximately 5 mm apart, and marked by sutures on each side. Perforation was confirmed by the green aiming beam, an audible change in the acoustic ablation signal, and by histologic analysis.

2.4 Data Analysis

A minimum of six perforations was made for each set of laser parameters. For the ex vivo tissue studies, ablation rates (μm/pulse) were defined as the sample thickness divided by the average number of pulses required to perforate the sample and recorded as the mean ± standard deviation (SD). The optical fiber tip was kept fixed in contact with the tissue during the ex vivo tissue experiments. For the in vivo studies, the optical fiber was advanced during ablation. The in vivo ablation results were recorded in terms of the number of pulses required to perforate the ureteral wall because it was not possible to control for the tissue wall thickness across different ureters and animals.

3. RESULTS

3.1 Ablation Rates

The Er:YAG ablation rates are shown in Figure 2 for the ex vivo tissue experiments. Perforation of the ureteral tissue samples was achieved at laser fluences of 3-5 J/cm^2 and pulse energies of 1.5 - 2.5 mJ, without advancing the fiber into the tissue. There was an almost two-fold increase in the ablation rate for a given fluence when reducing the laser pulse duration from 220 μs to 70 μs. The 220-μs line shows an ablation rate of 4 μm per J/cm^2, while the 70-μs line shows an ablation rate of 7 μm per J/cm^2. Reducing the pulse length to 8 μs produced a minor increase in the ablation rate, but at the expense of much lower laser energy output and peripheral mechanical tissue damage.

The in vivo ablation results are shown in Figure 3, plotted as the number of laser pulses to perforate the ureter, with the fiber advanced into the tissue during ablation. The ureteral wall was perforated with less than 20 pulses at a fluence of 3.6 J/cm^2 for all of the laser pulse lengths tested. At the lowest fluence of 1.8 J/cm^2, near the perforation threshold, the shorter laser pulse lengths were observed to be more efficient. This perforation threshold was lower than that observed for the ex vivo tissue experiments using thick or thin tissue samples.

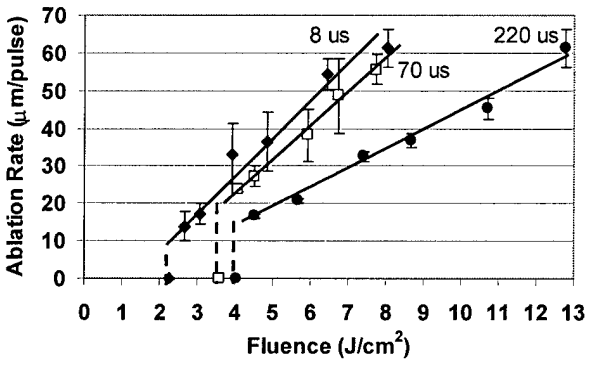

Figure 2. Er:YAG ablation rates for ex vivo ureter tissue using laser pulse lengths of 8, 70, 220 μs, and plotted as a function of laser fluence. Bars signify mean values ± S.D. (n=6). Note that the perforation threshold decreases as the laser pulse is decreased, and ablation is also more efficient.

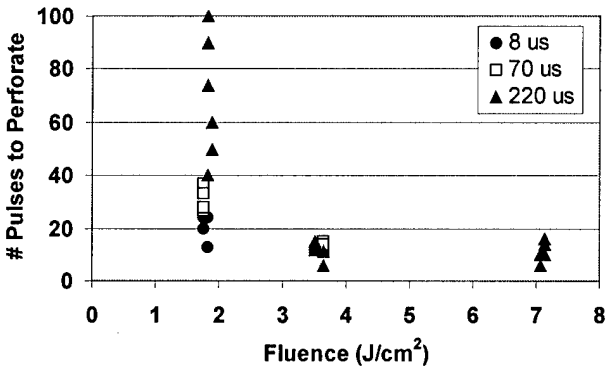

Figure 3. Er:YAG results for in vivo ureter ablation as a function of laser pulse length and fluence. The perforation threshold is approximately 1.8 J/cm^2, based on the increase in the number of pulses for perforation, and the large spread in the data points.

3.2 Thermal Damage Measurements

Histological measurements of thermal damage were conducted as a function of laser pulse duration. The results for the ex vivo tissue studies are shown in Figure 4. When the Er:YAG laser was operated in its normal long pulse mode (220 μs pulse length), a thermal damage zone of 30-60 μm was observed. Shortening the laser pulse to 70 μs resulted in a reduction of the thermal damage to 15-30 μm. The shortest laser pulse, measuring 8 μs, further reduced the thermal damage zone to 10-20 μm, but also resulted in a rougher cut, due to mechanical tissue-tearing effects.

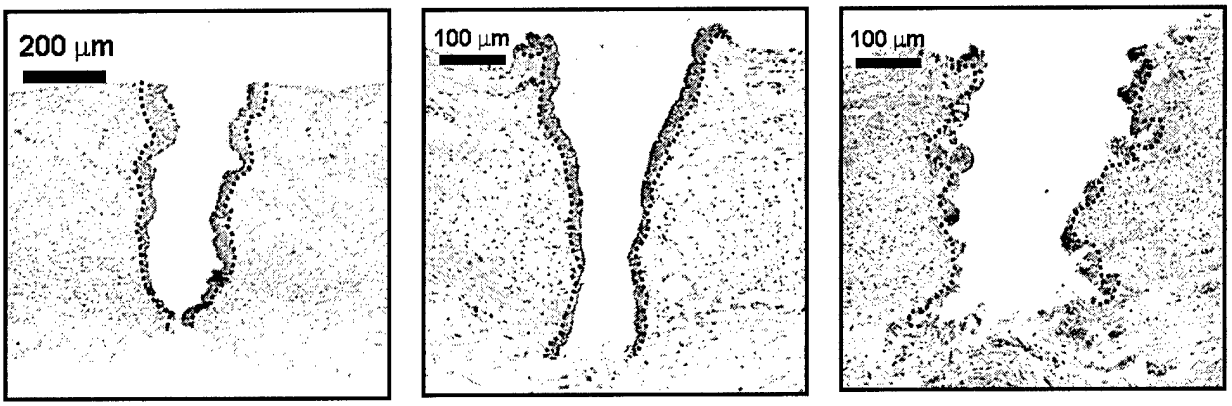

(a) 220 μs; Damage = 30-60 μm **(b)** 70 μs; Damage = 15-30 μm **(c)** 8 μs; Damage = 10-20 μm

Figure 4. Photomicrographs showing H&E stained histologic cross-sections of ureteral tissues ablated with the Er:YAG laser, ex vivo. The thermal damage zone decreases as the laser pulse duration is decreased. Rough, jagged borders of the ablation crater produced by 8 μs laser pulses may be due to mechanical tissue-tearing caused during ablation.

An ex vivo study was also performed to determine whether the thermal damage zone would increase with laser operation at higher pulse repetition rates, due to residual heat accumulation in the tissue with deposition of successive laser pulses. The pulse duration, energy per pulse, and total number of pulses were all kept constant at 70 μs, 10 mJ, and 20 pulses (total energy = 200 mJ), respectively, while the pulse repetition rate was varied from 10-30 Hz. The thermal damage zone increased as the laser pulse repetition rate increased, and a large increase in thermal damage was observed when the pulse repetition rate was increased from 20 to 30 Hz (Figure 5).

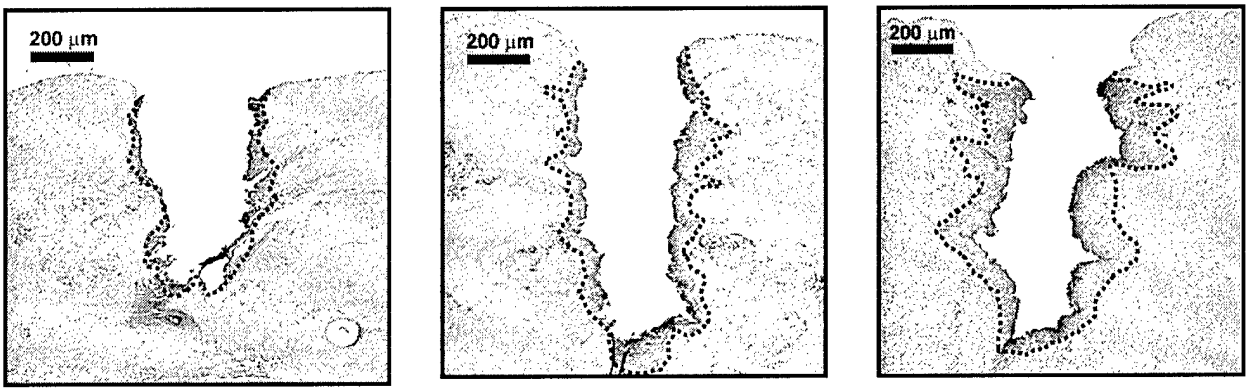

(a) 10 Hz; Damage = 20-40 μm **(b)** 20 Hz; Damage = 30-60 μm **(c)** 30 Hz; Damage = 60-120 μm

Figure 5. Photomicrographs showing H&E stained histologic cross-sections of urethral tissues ablated with the Er:YAG laser, ex vivo, with varying laser pulse repetition rates of 10–30 Hz. Energy was kept fixed at 10 mJ per pulse with a total of 20 pulses (200 mJ) delivered to the tissue. Note that there is a large increase in the thermal damage zone from 20 – 30 Hz, due to residual heat accumulation in the tissue during ablation. The dotted lines demarcate the border of the thermal damage zone.

The in vivo histological results are shown in Figure 6, for the 70 μs pulse duration. The thermal damage zone of 10-20 μm is slightly less than the 15-30 μm of thermal damage observed in the ex vivo tissue studies for 70 μs pulse lengths and considerably less than the 30-60 μm of thermal damage observed for the long pulse mode of 220 μs.

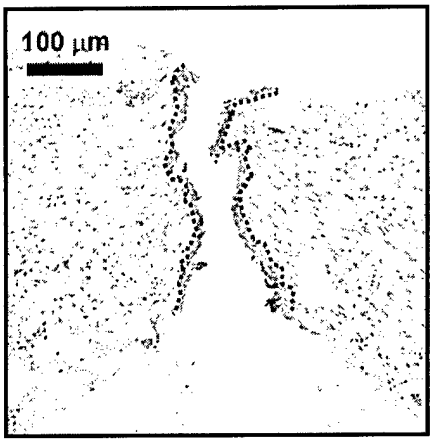

Figure 6. Photomicrographs showing H&E stained histologic cross-sections of ureteral tissue ablated with the Er:YAG laser, in vivo. The thermal damage zone measures 10-20 μm. The dotted lines demarcate the border of the thermal damage zone.

4. DISCUSSION

Success rates in treating strictures vary widely from 20-80 %, dependent on a variety of factors, including surgical technique and skill, type of stricture, scar tissue caused by previous treatment failures, patient follow-up and evaluation, and definition of stricture. While the use of the Ho:YAG laser has resulted in improved treatment of strictures, we hypothesize that the further reduction of peripheral thermal damage to the urethral or ureteral wall with Er:YAG laser incision may further improve these success rates. By operating at the 2.94 μm wavelength of the Er:YAG laser, and shortening the laser pulse length to approximately 70 μs, the thermal damage zone has been reduced to 10-20 μm, in vivo. This represents a 15-30 fold decrease in damage in comparison to the 300 μm of damage typically produced by the Ho:YAG laser, which is currently the laser of choice in urology.

This study has focused on the optimization of the Er:YAG laser for rapid and precise incision of urological tissues. Our results are similar to those of previous studies using the Er:YAG laser for ablation of other soft tissues. For example, reported threshold fluences of ablation for the long-pulse Er:YAG laser are 0.6-1.5 J/cm^2 for skin [32], ~ 2 J/cm^2 for aorta [33], ~ 1 J/cm^2 for retina [34], and ~ 1.8 J/cm^2 for the ureter reported here. Note that these low ablation thresholds also demonstrate that the Er:YAG laser is more efficient than the Ho:YAG laser, which has an ablation threshold of ~ 34 J/cm^2.

Thermal damage zones in other soft tissues for the long-pulse Er:YAG laser operated at low fluences (< 25 J/cm^2) have been reported to be 10-40 μm for skin [35], 10-20 μm for aorta [35], 20-40 μm for cornea [35], < 50 μm for trabecular tissue [36], 20-30 μm for retina [34], and 30-60 μm for ureter reported here. Mechanical tissue-tearing effects have also been observed in other tissues, e.g. aorta and cornea [35], and at pulse lengths of 50 μs and shorter [36]. Although we did not observe any mechanical tissue damage at the 70 μs pulse length, the 8-μs-pulse-length showed evidence of tissue shredding consistent with that observed in these previous studies.

Problems with the fiber tip "sticking" to the tissue during contact tissue ablation with the Er:YAG laser have also been previously reported [37,38]. This phenomenon was explained by the presence of overheated tissue debris at the fiber tip. During our preliminary in vivo experiments, however, we did not observe any "sticking" effects during advancement of the fiber into the ureter. This may be due to the use of different laser parameters, optical fibers, and/or tissues, and needs to be further studied.

In general, lower perforation thresholds, higher ablation rates, and less thermal damage were observed when progressing from ex vivo to in vivo experiments. Several factors may have contributed to these differences. First, the ability to advance the optical fiber into the tissue during in vivo ablation studies resulted in lower perforation thresholds and higher ablation rates for a given fluence. This occurred because the fluence at the tissue surface was not diminished due to divergence of the laser radiation at the output end of the fiber tip. Second, the decreased thermal damage seen in vivo may also be due to the level of hydration maintained in the tissue and absence of tissue desication which can occur during ex vivo tissue experiments.

5. CONCLUSIONS

The Er:YAG laser, operating at a pulse duration of ~ 70 μs, a fluence of 4 J/cm^2, and a repetition rate of 20 Hz, is capable of rapidly incising urethral and ureteral tissues, in vivo, with minimal thermal and mechanical side-effects. The Er:YAG laser is more efficient than the Ho:YAG laser for cutting ureteral and urethral tissues, with perforation thresholds measuring 2 J/cm^2 versus 34 J/cm^2, respectively. The Er:YAG laser is also more precise than the Ho:YAG laser, with peripheral thermal damage zones measuring 10-20 μm versus 300 μm, respectively. Chronic animal wound healing studies are planned to quantify scarring induced during Er:YAG laser incision, and optimization of mid-infrared fiber optic delivery systems for endoscopic laser delivery has begun.

ACKNOWLEDGMENTS

We would like to thank Jatuphon Chaiseesiri for his help in preparing the histology, and Ken Levin, Dan Tranh, and Alex Tchap of Infrared Fiber Systems, for providing the optical fibers used in these experiments.

This research was supported in part by the following grants and sponsors: laboratory start-up funding from the James Buchanan Brady Urological Institute; NIH Phase I SBIR awarded to Infrared Fiber Systems (Silver Spring, MD), Grant #1R43 EY13889-01; a Professional Development Award from the National Kidney Foundation of Maryland; and the Department of Defense Prostate Cancer Research Program, Grant #PC020586.

REFERENCES

1. R. V. Clayman, E. M. McDougall, S. Y. Nakada SY, "Endourology of the upper urinary tract: percutaneous renal and ureteral procedures," In: P. C. Walsh, A. B. Retik, E. D. Vaughan, A. J. Wein, eds. Campbell's Urology, 7th ed., Vol. 3, Philadelphia: WB Saunders. Pp. 2853-2863, 1998.
2. G. H. Jordan, S. M. Schlossberg, C. J. Devine, "Surgery of the penis and urethra," P. C. Walsh, A. B. Retik, E. D. Vaughan, A. J. Wein, eds. Campbell's Urology, 7th ed., Vol. 3, Philadelphia: WB Saunders, pp. 3341-3347, 1998.
3. M. A. Rosen, P. A. Nash, J. E. Bruce, J. W. McAninch, "The actuarial success rate of surgical treatment of urethral strictures," *J. Urol.*, vol. 151, p. 360A, 1994 (Abstract).
4. P. Albers, J. Fichtner, P. Bruhl, S. C. Muller, "Long-term results of internal urethrotomy," *J. Urol.*, vol. 156, pp. 1611-1614, 1996.
5. A. Benchekroun, A. Lachkar, A. Soumana, M. H. Farih, Z. Belahnech, M. Marzouk, M. Faik, "Internal urethrotomy in treatment of urethral stenoses (longterm results)," *Ann. Urol. (Paris)*, vol. 32, pp. 99-102, 1998.
6. C. F. Heyns, J. W. Steenkamp, M. L. De Kock, P. Whitaker, "Treatment of male urethral strictures: is repeated dilation or internal urethrotomy useful?" *J. Urol.*, vol. 160, pp. 356-358, 1998.
7. R. Klammert, P. Schneede, M. Kriegmair, "Die laserbehandlung von Harnrohrenstrikturen," *Urologie A*, vol. 33, pp. 295-298, 1994.
8. T. A. McNicholas, J. Colles, S. G. Bown, J. E. A. Wickham, "Treatment of urethral strictures with a prototype CO_2 laser endoscope," *Lasers Med. Sci.*, vol. 3, pp. 427, 1988.
9. W. C. Adkins, "Argon laser treatment of urethral stricture and vesical neck contracture," *Lasers Surg. Med.*, vol. 8, pp. 600-603, 1988.
10. H. Becker, J. Miller, H. D. Noske, J. P. Klask, W. Weidner, "Transurethral laser urethrotomy with argon laser: experience with 900 urethrotomies in 450 patients from 1978-1993," *Urol. Int.*, vol. 55, pp. 150-153, 1995.
11. A. Shanberg, R. Baghdassarian, L. Tansey, D. Sawyer, "K.T.P. 532 laser in treatment of urethral strictures," *Urology*, vol. 32, pp. 517-520, 1988.
12. P. J. Turek, T. R. Malloy, M. Cendron, V. L. Carpiniello, A. J. Wein, "KTP-532 laser ablation of urethral strictures," *Urology*, vol. 40, pp. 330-334, 1992.
13. J. A. Smith JA, Dixon JA, "Neodymium:YAG laser treatment of benign urethral strictures," *J. Urol.*, vol. 131, pp. 1080-1081, 1984.
14. J. A. Smith, "Treatment of benign urethral strictures using a sapphire tipped neodymium:YAG laser," *J. Urol.*, vol. 142, pp. 1221-1222, 1989.
15. P. N. Dogra, G. Nabi, "Core-through urethrotomy using the neodymium:YAG laser for obliterative urethral strictures after traumatic urethral disruption and/or distraction defects: long-term outcome," *J. Urol.*, vol. 167, pp. 543-546, 2002.

16. G. Nabi, P. N. Dogra, "Endoscopic management of post-traumatic prostatic and supraprostatic strictures using Neodymium-YAG laser," *Int. J. Urol.*, vol. 9(12), pp. 710-714, 2002.
17. R. K. Singal, J. D. Denstedt, H. A. Razvi, S. S. Chun, "Holmium:YAG laser endoureterotomy for treatment of ureteral stricture," *Urology*, vol. 50, pp. 875-880, 1997.
18. G. S. Gerber, D. Kuznetzov, J. A. Leef, J. Rosenblum, G. D. Steinberg, "Ho:YAG laser endoureterotomy in the treatment of ureteroenteric strictures following orthotopic urinary diversion," *Tech. Urol.*, vol. 5, pp. 45-48, 1999.
19. H. Hibi, K. Mitsui, T. Taki, H. Mizumoto, Y. Yamamda, N. Honda, H. Fukatsu, "Holmium laser incision technique for ureteral stricture using a small-calibre ureteroscope," *J.S.L.S.*, vol. 4, pp. 214-220, 2000.
20. A. R. Kural, E. R. Coskuner, I. Cevik, "Holmium laser ablation of recurrent strictures of urethra and bladder neck: preliminary results, *J. Endourol.*, vol. 14, pp. 301-304, 2000.
21. B. A. Laven, R. C. O'Connor, G. D. Steinberg, G. S. Gerber, "Long-term results of antegrade endoureterotomy using the holmium laser in patients with ureterointestinal strictures," *Urology*, vol. 58, pp. 924-929, 2001.
22. J. Kourambas, F. C. Delvecchio, G. M. Preminger, "Low-power holmium laser for the management of urinary tract calculi, strictures, and tumors," *J. Endourol.*, vol. 15(5), pp. 529-32, 2001.
23. K. Matsuoka, M. Inoue, S. Iida, K. Tomiyasu, S. Noda, "Endoscopic antegrade laser incision in the treatment of urethral stricture," *Urology*, vol. 60(6), pp. 968-972, 2002.
24. J. D. Watterson, M. Sofer, T. A. Wollin, L. Nott, J. D. Denstedt, "Holmium:YAG laser endoureterotomy for ureterointestinal strictures," *J. Urol.*, vol. 167(4), pp. 1692-1695, 2002.
25. H. Baur, W. Schneider, J. E. Altwein, "Treatment of recurrent urethral strictures by photoablation with the EXCIMER laser," *B.A.U.S.*, vol. 118, 1992 (Abstract).
26. M. Anidjar, P. Mongiat-Artus, J. P. Broulard, P. Meria, P. Teillac, A. Le Duc, P. Berthon, O. Cussenot, "Thermal radiofrequency induced porcine ureteral stricture: a convenient endourologic model," *J. Urol.*, vol. 161, pp. 298-303, 1999.
27. P. Meria, M. Anidjar, J. P. Brouland, P. Teillac, A. Le Duc, P. Berthon, O. Cussenot, "An experimental model of bulbar urethral stricture in rabbits using endoscopic radiofrequency coagulation," *Urology*, vol. 53, pp. 1054-1057, 1999.
28. J. M. H. Teichman, K. F. Chan, P. P. Cecconi, N. S. Corbin, A. D. Kamerer, R. D. Glickman, A. J. Welch, "Er:YAG versus Ho:YAG lithotripsy," *J. Urol.*, vol. 165, pp. 876-879, 2001.
29. K. F. Chan, H. Lee, J. H. M. Teichman, A. D. Kamerer, H. S. McGuff, G. Vargas, A. J. Welch, "Erbium:YAG laser lithotripsy mechanism," *J. Urol.*, vol. 168(2), pp. 436-441, 2002.
30. N. M. Fried, "Potential applications of the Erbium:YAG laser in endourology," *J. Endurol.*, vol. 15(9), pp. 889-894, 2001.
31. N. M. Fried, G. M. Long, "Erbium:YAG laser ablation of urethral and ureteral tissues," *Proc. S.P.I.E.: Lasers in Urology*, vol. 4609, pp. 122-127, 2002.
32. J. T. Walsh, T. F. Deutsch, "Er:YAG laser ablation of tissue: measurement of ablation rates," *Lasers Surg. Med.*, vol. 9, pp. 327-337, 1989.
33. J. T. Walsh, "Pulsed ablation of tissue: analysis of the removal process and tissue healing," Ph.D. Thesis. Northwestern University, Evanston, IL. 1988.
34. T. Wesendahl, P. Janknecht, B. Ott, M. Frenz, "Erbium:YAG laser ablation of retinal tissue under perfluorodecaline: determination of laser-tissue interaction in pig eyes," *Invest. Ophthalmol. Vis. Sci.*, vol. 41, pp. 505-512, 2000.
35. J. T. Walsh, T. J. Flotte, T. F. Deutsch, "Er:YAG laser ablation of tissue: effect of pulse duration and tissue type on thermal damage," *Lasers Surg. Med.*, vol. 9, pp. 314-326, 1989.
36. R. A. Hill, D. Stern, M. L. Lesiecki, J. Hsia, M. W. Berns, "Effects of pulse width on erbium:YAG laser photothermal trabecular ablation (LTA)," *Lasers Surg. Med.*, vol. 13, pp. 440-446, 1993.
37. S. Sporri, M. Frenz, H. J. Altermatt, H. U. Bratschi, V. Romano, M. Forrer, E. Dreher, H. P. Weber, "Effects of various laser types and beam transmission methods on female organ tissue in the pig: an in vitro study," *Lasers Surg. Med.*, vol. 14, pp. 269-277, 1994.
38. P. D. Brazitkos, D. J. D'Amico, T. W. Bochow, M. Hmelar, G. R. Marcellino, N. T. Stangos, "Experimental ocular surgery with a high-repetition-rate erbium:YAG laser," *Invest. Ophthalmol. Vis. Sci.*, vol. 39, pp. 1667-1675, 1998.

Proc. SPIE: Lasers in Urology In Press.

APPENDIX 4

Assembly and Testing of Germanium / Silica Optical Fibers for Flexible Endoscopic Delivery of Erbium:YAG Laser Radiation

Charles A. Chaney, Yubing Yang, Nathaniel M. Fried*
Dept. of Urology, Johns Hopkins Medical Institutions, Baltimore, MD 21224

ABSTRACT

Endoscopic applications of the Erbium:YAG laser have been limited due to the lack of an optical fiber delivery system that is robust, flexible, and biocompatible. This study reports the assembly and testing of hybrid optical fibers consisting of 1-cm-length, 550-micron-core, silica fiber tips attached to either 350-micron or 425-micron germanium oxide "trunk" fibers. Er:YAG laser radiation with a wavelength of 2.94 microns, pulse lengths of 70 and 220 microseconds, repetition rates of 3-10 Hz, and laser output energies of up to 300 mJ was delivered through the fibers for testing. Maximum fiber output energies measured 180 $\pm$ 30 mJ and 82 $\pm$ 20 mJ (n=10) under straight and tight bending configurations, respectively, before fiber interface damage occurred. By comparison, the damage threshold for the germanium fibers without silica tips during contact soft tissue ablation was only 9 mJ (n=3). Studies using the hybrid fibers for lithotripsy also resulted in fiber damage thresholds (55-114 mJ) above the stone ablation threshold (15-23 mJ). Hybrid germanium / silica fibers represent a robust, flexible, and biocompatible method of delivering Er:YAG laser radiation during contact soft tissue ablation. Significant improvement in the hybrid fibers will be necessary before their use in Er:YAG laser lithotripsy.

Key Words: ablation, erbium, holmium, laser, lithotripsy, stricture, ureter, urethra

1. INTRODUCTION

The Erbium:YAG laser has been used extensively for precise tissue ablation in medical fields which do not require a flexible optical fiber delivery system, such as dermatology [1,2], dentistry [3,4], and ophthalmology [5-11]. In these fields, the use of an articulated arm delivery system or semi-rigid optical fibers is adequate for performing surgery. However, for medical applications requiring delivery of laser radiation through a flexible endoscope, such as the upper urinary tract, current optical fibers and waveguides for the Er:YAG laser remain inadequate.

Although there are several types of optical fibers and waveguides available for delivery of mid-infrared laser radiation, including chalcogenide, zirconium fluoride, sapphire, germanium oxide, and hollow silica waveguides, all of these delivery systems have major limitations [12-14]. The chalcogenide fibers cannot handle high power, they are toxic, and they break easily. The zirconium fluoride fibers are also brittle, hygroscopic, and toxic in tissue. The sapphire fibers suffer from mechanical stress and breakage during tight bending conditions. The germanium oxide fibers have a low melting temperature preventing their use in contact mode at high powers. The hollow silica waveguides are not biocompatible and have limited bending ability with high transmission losses during tight bending. Thus, the ideal mid-infrared optical fiber that combines high-power delivery, flexibility, chemical and mechanical durability, and biocompatibility, has yet to be developed.

The goal of this study is to test a hybrid optical fiber with the Erbium:YAG laser, which combines the high-power transmission and flexibility of the germanium oxide fiber with the robust and biocompatible low-OH silica fiber tips currently in clinical use with the Holmium:YAG laser. Although increased absorption limits the use of long low-OH silica fibers beyond wavelengths of approximately 2.5 μm, previous studies have demonstrated that short low-OH silica fiber lengths, on the order of a few centimeters, are capable of transmitting sufficient Er:YAG laser energy for soft tissue ablation [5,6,8,15]. This study demonstrates that long hybrid fibers are capable of being assembled with a simple process that reduces many of the limitations associated with current mid-IR optical fibers, and that sufficient Er:YAG laser energy can be transmitted through these fibers during insertion into a flexible endoscope for use in applications requiring soft and hard tissue ablation.

*nfried@jhmi.edu; phone: 1 410 550 7906; fax: 1 410 550 3341

2. MATERIALS AND METHODS

2.1 Laser Parameters

An Erbium:YAG laser (SEO 1-2-3, Schwartz Electro-Optics, Orlando, FL) operating at a wavelength of 2.94 μm was connected to either a fixed long-pulse laser power supply (220-μs-pulse length, 400 mJ/pulse) or a variable pulse width laser power supply (Model 8800V, Analog Modules, Longwood, FL), producing up to 30 mJ per pulse at 70-μs-pulse-lengths. The laser radiation was externally focused with a 50-mm-focal-length calcium fluoride lens into either 250, 350, or 425-μm-core germanium oxide optical fibers (Infrared Fiber Systems, Silver Spring, MD), with and without low-OH silica fiber tips attached to the output end of the germanium "trunk" fiber. Fiber output energy was measured using a pyroelectric detector (Gentec ED-200, Ste.-Foy, Quebec), and the laser pulse duration was measured using a photovoltaic infrared detector (PD-10.6, Boston Electronics, Brookline, MA).

2.2 Germanium "Trunk" Fibers

Preliminary laser ablation tests were conducted with 250-μm-core and 425-μm-core germanium oxide fibers in direct contact with ex vivo hard and soft tissue samples, including porcine ureters, and uric acid and calcium oxalate monohydrate (COM) stones. A total of 500 pulses were delivered to the tissue. Pre- and post-ablation fiber output energies were measured to determine whether any damage occurred to the fiber tip. An optical microscope was used to analyze the output ends of the germanium fibers for evidence of fiber tip degradation after contact tissue ablation.

2.3 Hybrid Fiber Assembly

The hybrid fiber consisted of a 1-cm-long, 550-μm-core, low-OH silica fiber tip attached to either a 350-μm- or 425-μm germanium trunk fiber. For the initial fiber preparation, the germanium fiber jacket was softened using chemical treatment (1-methyl-2-pyrrolidinone at 150 °C for 2 min. then isopropanol for 3 min.) and then stripped with a razor blade. The germanium and silica fibers were polished with rough 600-grit and then fine 5-micron sandpaper. The fibers were then aligned under a microscope using a laboratory-constructed mechanical setup.

Several different methods of attachment were explored (Figures 1 and 2). First, index-matching UV-cured optical epoxy (Norland, New Brunswick, NJ) was applied with a syringe needle either around the fibers or at the fiber interface (n = 10 fibers). Second, 30-gauge PTFE heat shrink tubing (normal ID=850 μm, shrunk ID=375 μm, wall thickness = 150 μm, length = 5 mm) was shrunk around the germanium/silica fiber interface using a heat gun (n = 10 fibers). The PTFE tubing (Small Parts, Miami Lakes, FL) also served the purpose of acting as a biocompatible jacket surrounding any exposed germanium fiber. Third, stainless steel hypodermic tubing (Small Parts, ID=0.675 mm, OD=1.05 mm) was used to align the fibers (n = 5 fibers). Fourth, glass capillary tubing (VitroCom, Mountain Lakes, NJ, ID=0.7 mm, OD=0.87 mm) was used for fiber attachment. Two attachment methods were explored: with the fibers in contact at the interface (n = 10 fibers) or with an air gap (~200 μm) at the interface (n = 10 fibers).

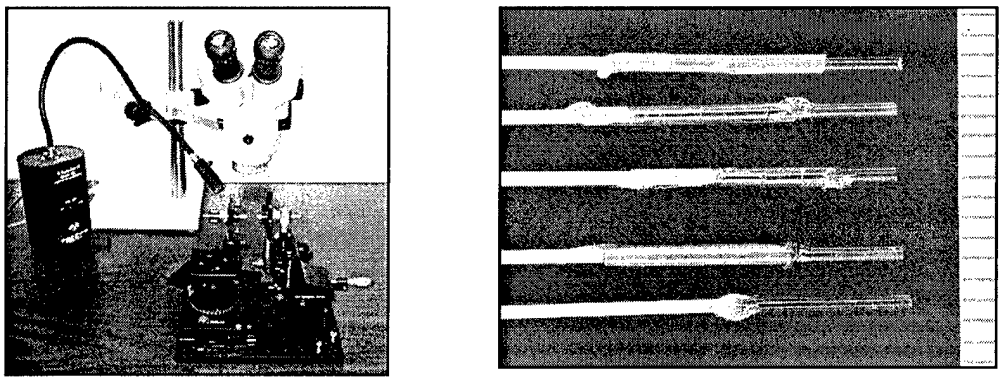

(a) (b)

Figure 1. (a) Experimental setup used to assemble the hybrid fibers. (b) Image of the germanium / silica hybrid fibers assembled using 5 different methods: (1) heat-shrink tubing, (2) glass capillary tubing, (3) glass tubing with an air gap at the fiber interface, (4) stainless steel hypodermic tubing, and (5) UV-cured optical epoxy. For all of the methods, an approximately 1 cm-long, 550-mm-core, low-OH silica tip was attached to a 425-mm-core germanium trunk fiber. Ball-shaped glue drops are present in Figures b-e at the interface between the yellow germanium jacket and the conduit material and at the interface between the silica tip and the conduit. The ruler lines = 1 mm.

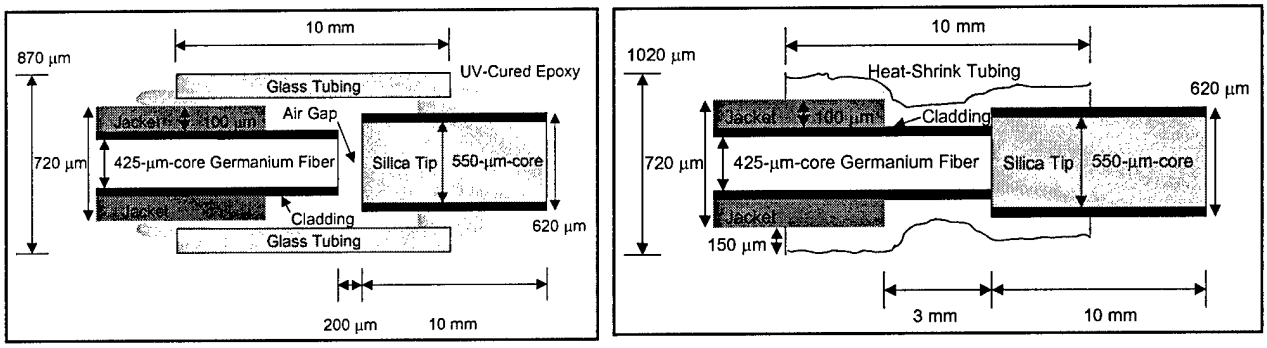

Figure 2. Diagrams of the dimensions of the 425/550 hybrid fiber assembled using (a) heat shrink tubing, and (b) glass capillary tubing with epoxy and an air gap at the germanium / silica interface.

2.4 Fiber Transmission and Bending Tests

Preliminary fiber bending tests were conducted with germanium and sapphire optical fibers, ranging in core diameter from 150 – 500 µm. The fibers were inserted into a 15 Fr flexible cysto-urethroscope with a 7 Fr working channel. Basic fiber testing was performed to determine whether the fiber could withstand high mechanical stress under tight bending conditions and whether the fiber presence hindered maximum deflection of the scope. Peak Er:YAG energy transmission through the hybrid fibers was then measured for both straight and bent configurations.

2.5 Stone Ablation Studies

Limited studies were also performed with the Er:YAG laser and the hybrid (350/550 and 425/550) fibers for contact tissue ablation of urological stones. The goal of these studies was to demonstrate that sufficient energy could be delivered through the hybrid fibers in contact mode for endoscopic stone ablation. Human uric acid and calcium oxalate monohydrate stones were obtained from a stone analysis laboratory (UroCore LabCorp, Oklahoma City, OK), sectioned with a water-cooled band saw into cylindrical samples (~ 10-mm-diameter), and then weighed with an analytical balance (dry weight = 300-450 mg). The stone samples were then placed in a water bath, and the hybrid fiber tip placed in contact with the stone. Er:YAG laser radiation was delivered to the stone with pulse lengths of 220 µs, pulse repetition rates of 3 Hz, and fiber output energies of from 5-150 mJ.

2.6 Data Analysis

For the fiber damage studies, a total of 500 laser pulses was delivered through the fiber at each energy level between pre- and post-testing measurements. For the bare germanium fibers, the measurements were done during contact soft tissue ablation and represented the fiber tip damage threshold. For the hybrid fiber testing, measurements were initially made in air and then in contact with the stone samples. Maximum fiber output energy was recorded as the mean $\pm$ standard deviation (S.D.) for N samples tested. Statistical analysis was conducted between the data sets for maximum pulse energies achieved with each method of hybrid fiber assembly. ANalysis Of Variance (ANOVA) was used to determine statistical significance between data sets ($P < 0.05$ was considered statistically significant).

3. RESULTS

3.1 Germanium Trunk Fibers

Preliminary laser ablation tests were conducted with 250-µm-core and 425-µm-core germanium oxide fibers in direct contact with ex vivo samples of hard and soft urological tissues. The fiber damage thresholds for the soft tissue studies were 4 mJ (7 J/cm^2) and 9 mJ (6 J/cm^2) for the 250 µm and 425 µm fibers, respectively (Figure 3). These values are above the threshold for perforating samples of ureteral tissue, 2 mJ (4.1 J/cm^2) and 5.1 mJ (3.7 J/cm^2), respectively [16]. For the hard tissue studies, the fiber damage thresholds measured 12 mJ and 30 mJ (22 J/cm^2), for the uric acid and COM stones, respectively (Figure 4). These results demonstrate that the germanium oxide fiber is capable of ablating soft and hard tissues without fiber tip damage. However, the fiber is limited to operation at relatively low laser energies during contact tissue ablation, which may not be practical for clinical applications requiring rapid and efficient tissue ablation.

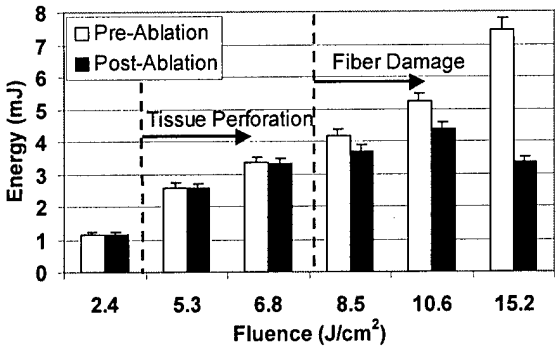

(a) Ureter, 250 μm fiber

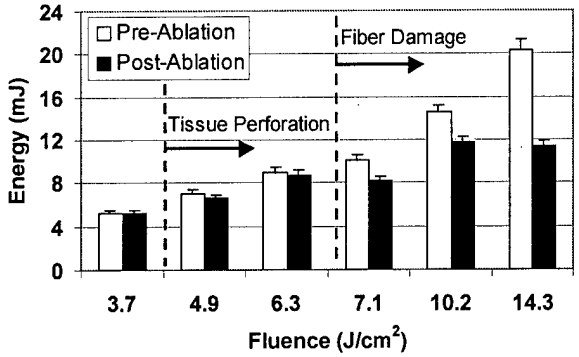

(b) Ureter, 425 μm fiber

Figure 3. Germanium oxide fiber damage thresholds for (a) 250-μm-core fibers, and (b) 425-μm-core fibers, placed in direct contact with soft ureteral tissue. A total of 500 pulses were delivered with a pulse length of 70 μs and a pulse repetition rate of 10 Hz. Error bars signify a ± 5% variation in pulse to pulse energy stability.

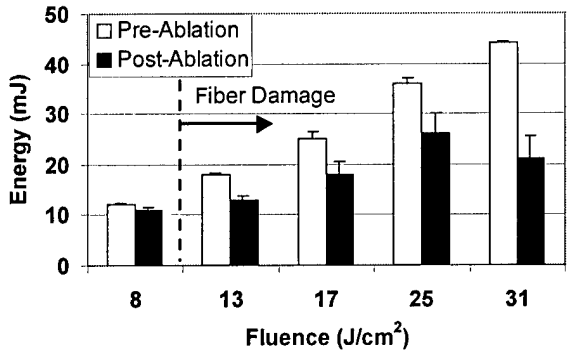

(a) Uric Acid stone, 425 μm fiber

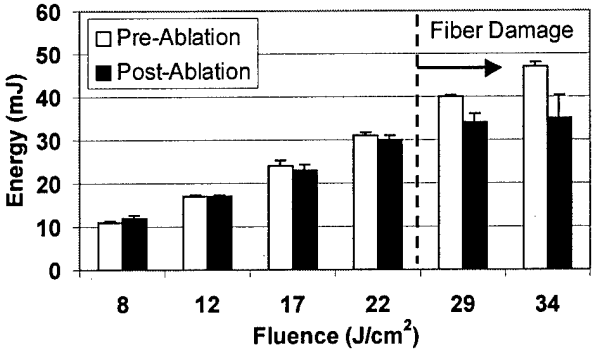

(b) COM stone, 425 μm fiber

Figure 4. Germanium oxide fiber damage thresholds for 425-μm-core fibers placed in contact with (a) uric acid stones, and (b) calcium oxalate monohydrate stones. A total of 500 pulses were delivered with a pulse length of 220 μs and pulse repetition rate of 3 Hz. Error bars represent mean ± standard deviation (n = 4).

The primary mechanism of germanium fiber damage during contact tissue ablation is melting of the fiber tip due to the high ablative temperatures. Figure 5 shows the fiber tips at different stages of meltdown, beginning with a normal tip surface, then particle formation, cracking and charring, and finally catastrophic meltdown with crystalline formation. During these progressive phases of fiber degradation, the fiber output energy also steadily dropped.

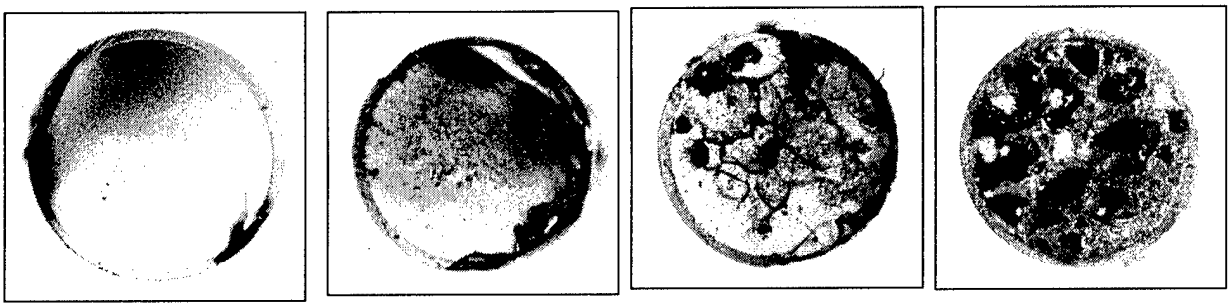

(a) (b) (c) (d)

Figure 5. Mechanism of germanium oxide fiber tip damage when tested in contact with tissue. (a) normal fiber tip, (b) particulate formation on the fiber tip, (c) cracking and charring, and (d) crystalline formation. The progressive deterioration is due to melting of the fiber tip when in contact with the tissue during high-temperature tissue ablation. Fiber tip damage was not observed during non-contact ablation studies. The parameters were: 425-μm-core fiber, 10 mJ/pulse, 70-μs-pulse duration, 10 Hz pulse repetition rate, and a total of 500 pulses.

There was no evidence of fiber damage when the germanium fibers were used previously for tissue ablation in non-contact mode. These trunk fibers have transmitted up to 20 Watts (2 Joules at 10 Hz) without problem [17].

3.2 Hybrid Germanium / Silica Fibers

To overcome the limitations of the germanium fiber for contact tissue ablation, a hybrid fiber consisting of a short low-OH silica fiber tip was attached to the germanium trunk fiber using several different methods. Table 1 shows the average output energy transmitted through the fiber for each of these methods before a drop in output energy was observed due to damage at the germanium / silica interface. The damage threshold for the germanium fiber without silica tip during contact soft tissue ablation is also included for comparison. Using the heat-shrink tubing method, hybrid fiber output energies measured 180 $\pm$ 30 mJ (76 $\pm$ 13 J/cm^2), before fiber damage was observed (n=10).

Table 1. Comparison of results for different materials and methods used to construct germanium / silica hybrid fibers.

Assembly Method[a]	Maximum Pulse Energy (mJ)	N
Germanium tip only[b]	9 $\pm$ 1	3
Silica tip attached with:		
UV-cured epoxy	10 $\pm$ 5	10
Steel hypodermic tubing	109 $\pm$ 47	10
Glass capillary tubing:		
with air gap at interface	104 $\pm$ 38	10
without air gap at interface	139 $\pm$ 49	10
Heat-shrink tubing	180 $\pm$ 30	10

[a] All fibers were constructed using a 425-μm-core germanium trunk fiber and a 1-cm-long, 550-μm-core silica fiber tip. The fibers were tested using an Er:YAG laser with a 220 μs laser pulse length at 3 Hz.

[b] Values for the germanium fibers without silica tip represent maximum pulse energies achieved during contact soft tissue ablation. No problems were encountered during non-contact ablation.

3.3 Fiber Bending and Transmission Tests

Earlier tests showed that the sapphire optical fibers were more robust than the germanium fibers, as evidenced by the difference in their melting temperatures (2030 °C versus 680 °C) and the absence of fiber tip damage during contact soft tissue ablation [12, 18]. However, the sapphire fiber was not pursued further because both 250-μm- and 425-μm-core sapphire fibers suffered multiple fractures upon insertion into the flexible cysto-urethroscope under tight bending conditions (Table 2). While the 425-μm-core germanium fibers also fractured upon repeated bending, the 150-μm-, 250-μm-, and 350-μm-core germanium fibers suffered no mechanical damage under similar test conditions. Figure 6 shows a 350-μm-core germanium oxide fiber inserted through the 7 Fr working channel of a 15 Fr flexible cysto-urethroscope. The scope was deflected at a maximum angle corresponding to a bend radius of approximately 15 mm with and without the fiber inserted.

Table 2. Bending tests performed using a 15 Fr flexible cysto-urethroscope with 7 Fr working channel and ~ 15 mm bend radius.

Fiber Type / Core Size	Minimum Bend Radius[a]	Flexible Scope Breaking Test
Sapphire		
150 μm	20 mm	Passed
250 μm	30 mm	Failed
325 μm	60 mm	Not tested
425 μm	80 mm	Failed
Germanium Oxide		
150 μm	5 mm	Passed
250 μm	10 mm	Passed
350 μm	15 mm	Passed
425 μm	25 mm	Failed
500 μm	40 mm	Failed

[a] Minimum bend radius values are taken from commercial literature (www.photran.com and www.infraredfibersystems.com).

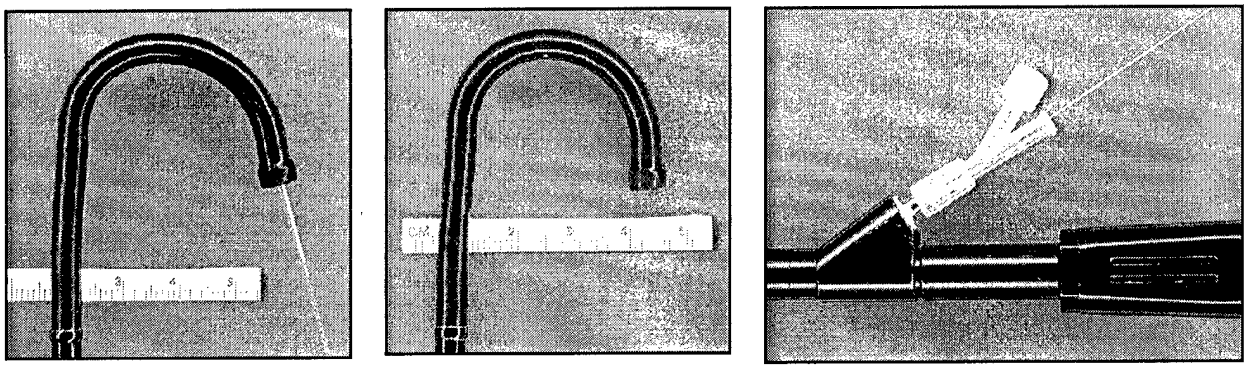

(a) (b) (c)

Figure 6. Images of a 350-μm-core germanium / silica hybrid fiber inserted through a 15 Fr flexible cysto-urethroscope with a 7 Fr working channel. (a) The fiber is bent to a ~ 15-mm bend radius without breaking under maximum scope deflection. (b) Maximum deflection of the scope without fiber present also corresponds to a ~ 15-mm bend radius, demonstrating that the fiber does not hinder scope deflection. (c) The fiber is successfully inserted at a 30-degree angle into the working channel.

Both the 350/550 and 425/550 germanium/silica hybrid fibers showed a significant decrease in energy output when bent to just above their minimum bending radius, 15 mm for the 350 μm trunk fiber and 25 mm for the 425 μm trunk fiber (Table 3). The damage mechanism was usually observed as sparking at the germanium/silica fiber interface, resulting in a melting of the germanium surface at the fiber interface, and noted as an immediate loss in energy greater than 5%. The difference in results between the 250-, 350-, and 425-μm trunk fibers can be explained in part by the difference in the cross-sectional area at the germanium fiber tip. Assuming the melting temperature of the germanium fiber tip at the interface is the limiting factor, the maximum fluence that the interface can handle before melting is a function of both energy and fiber diameter. Thus, a larger trunk fiber diameter transmits greater energy, as observed in Table 3.

Table 3. Damage thresholds during germanium / silica fiber bending tests.

Fiber Core (μm) (Trunk / Tip)	Maximum Energy (mJ) Straight	Bent	Bend Radius (mm)	N
425 / 550	180 ± 30	82 ± 20	30	10
350 / 550	93 ± 13	65 ± 20	20	10
250 / 365	27 ± 8	28 ± 9	20	8

3.4 Lithotripsy Studies

Both the 350/550 and 425/550 hybrid germanium/silica fibers were tested for Er:YAG laser ablation of uric acid and calcium oxalate monohydrate (COM) stones. The ablation threshold for the stones and the peak energies transmitted through the fibers before fiber interface damage occurred was measured (Table 4). Ablation craters were first observed in the stones at energy levels of 15-23 mJ. There was no statistically significant dependence on stone type or trunk fiber used. The peak energies, however, were again dependent on fiber trunk diameter (350 or 425 μm), similar to the previous results for the fiber bending studies.

Table 4. Results using hybrid germanium / silica fibers for Er:YAG lithotripsy.

Fiber Core (μm) (Trunk / Tip)	Stone Type	Stone Ablation Threshold (mJ)	Fiber Damage Threshold (mJ)	N
350/550	uric acid	15 ± 2	55 ± 8	3
	COM*	22 ± 5	63 ± 11	3
425/550	uric acid	19 ± 1	90 ± 32	4
	COM	23 ± 9	114 ± 8	4

*COM = calcium oxalate monohydrate

4. DISCUSSION

Several applications in urology may benefit from the availability of a suitable optical fiber for tissue ablation using the Erbium:YAG laser. Potential applications include more precise laser incision of ureteral and urethral strictures and more efficient laser lithotripsy. Previous studies by our research group suggest that Er:YAG laser incision of the ureter and urethra reduces peripheral thermal damage by a factor of 10 in comparison with the Ho:YAG laser (30 $\pm$ 10 μm vs. 290 $\pm$ 30 μm), which may translate into less scarring and improved success rates [14,16,18].

Teichmann, et al, have reported that Er:YAG laser lithotripsy is approximately 2.4 times more efficient than Ho:YAG laser lithotripsy, and that the lack of a reliable optical fiber delivery system is the major limitation to clinical application of Er:YAG laser lithotripsy [19]. They demonstrated that both the 425-μm-core sapphire and germanium fibers suffered significant degradation during Er:YAG laser lithotripsy studies, with fiber output energies declining to less than 70% of their initial 100 mJ and 200 mJ energies, respectively. Other experiments with the sapphire fiber were limited to energies of 50 mJ to minimize fiber damage [21].

Recently, Papagiakoumou, et al, have also reported the characterization of the germanium oxide fibers for flexible transmission of Er:YAG laser radiation [22]. They reported that the fibers exhibited no significant bending losses when bent to a radius of 40 mm and transmitting up to 20 mJ of energy. While these testing conditions were different than those of the current study (e.g. no silica tip, lower energy transmission, and higher bend radius), they nevertheless further demonstrate the potential of the germanium fiber as a flexible delivery system.

When comparing our methods used to assemble the hybrid fibers, it should be noted that there was a large difference in peak output energy between some of the methods. The bare germanium fibers and hybrid fibers attached with epoxy performed poorly in comparison with the hybrid fibers attached with metal, glass, and heat-shrink tubing. This can be explained again by considering the low melting temperature of the germanium fiber. The epoxy presumably acted as an absorbing material, resulting in thermal buildup at the interface, and eventual fiber decay and transmission loss. On the contrary, the heat-shrink and glass tubing were more efficient in transmitting coupling losses at the fiber interface through the wall, resulting in less thermal buildup. The alignment of the germanium / silica fiber interface inside the steel tubing was difficult because the material was not transparent.

The performance of the hybrid fibers was also limited when the fibers were placed either in tight bending configurations or in contact with hard tissue (e.g. stones). Some of the fiber damage and transmission losses may be due to limitations in the spatial and temporal beam quality of the input laser beam and the introduction of higher modes during bending. Future research will focus on delivering a single mode Gaussian or flat-top spatial beam profile and eliminating the micro-pulse spikes that compose the Er:YAG temporal beam profile [16].

Overall, our results show that by adding a robust silica fiber tip to the germanium fiber, fiber output energies may be increased to 180 $\pm$ 30 mJ (76 $\pm$ 13 J/cm^2) and 82 $\pm$ 20 mJ (35 $\pm$ 9 J/cm^2), in straight and tight bending configurations, respectively, without fiber damage. This represents a large improvement over the 9 mJ (6 J/cm^2) peak energy achieved during testing of the bare germanium fiber in contact with soft tissue (Figure 3b). While these results demonstrate that the hybrid germanium / silica fiber currently transmits sufficient energy for contact soft tissue ablation through a flexible endoscope, further improvements will be necessary before the hybrid fiber can be used effectively for Er:YAG laser lithotripsy. These fiber output energies are still too low to efficiently ablate stones at a rate suitable for clinical use. We are currently working to further refine our hybrid fiber assembly method to provide even higher and more consistent Er:YAG laser output energy and smaller, more flexible fibers for use in flexible endoscopes.

5. CONCLUSIONS

A robust, flexible, and biocompatible hybrid germanium / silica fiber was assembled capable of delivering Erbium:YAG laser radiation through a flexible endoscope. This fiber may serve as a reliable delivery system with the Er:YAG laser for applications in the urological tract which may benefit from more precise and efficient laser ablation. Such applications may include laser ablation of urethral and ureteral strictures and laser lithotripsy. Assembly of smaller diameter hybrid fibers, more rigorous endoscope bending tests, and achievement of higher fiber output energy thresholds will all be pursued in the further development and testing of these hybrid fibers.

ACKNOWLEDGMENTS

We thank Ken Levin, Dan Tranh, and Alex Tchap of Infrared Fiber Systems, for providing the germanium fibers used in this study. This research was supported in part by the following sponsors: The Brady Urological Institute of Johns Hopkins Medical School; an NIH Phase I SBIR grant awarded to Infrared Fiber Systems (Silver Spring, MD), Grant #1R43 EY13889-01; a Professional Development Award from the National Kidney Foundation of Maryland; a New Investigator Award from the Department of Defense Prostate Cancer Research Program, DAMD17-03-0087; a grant from the A. Ward Ford Memorial Institute (American Society for Laser Medicine and Surgery).

REFERENCES

1. R. Kaufmann, "Role of the Erbium:YAG laser in the treatment of aged skin," *Clin. Exp. Dermatol.*, vol. 26(7), pp. 631-636, 2001.
2. T. S. Alster, J. R. Lupton, "Er:YAG cutaneous laser resurfacing," *Dermatol. Clin.*, vol. 19, pp. 453-466, 2001.
3. P. Rechmann, D. S. Glodin, T. Hennig, "Er:YAG lasers in dentistry: an overview," *Proc. S.P.I.E.: Lasers Dent. IV*, vol. 3248, pp. 2-13, 1998.
4. D. M. Clarkson, "A review of technology and safety aspects of erbium lasers in dentistry," *Dent. Update*, vol. 28(6), pp. 298-302, 2001.
5. S. A. Ozler, R. A. Hill, J. J. Andrews, G. Baerveldt, M. W. Berns, "Infrared laser sclerostomies," *Invest. Ophthalmol. Vis. Sci.*, vol. 32(9), pp. 2498-2503, 1991.
6. R. A. Hill, G. Baerveldt, S. A. Ozler, M. Pickford, G. A. Profeta, M. W. Berns, "Laser trabecular ablation (LTA)," *Lasers Surg. Med.*, vol. 11(4), pp. 341-346, 1991.
7. M. L. McHam, D. L. Eisenberg, J. S. Schuman, N. Wang, "Erbium:Yag laser trabecular ablation with a sapphire optical fiber," *Exp. Eye Res.*, vol. 65, pp. 151-155, 1997.
8. G. Stevens Jr, B. Long, J. M. Hamann, R. C. Allen, "Erbium:YAG laser-assisted cataract surgery," *Ophthalmic Surg. Lasers*, vol. 29(3), pp. 185-189, 1998.
9. P. D. Brazitkos, D. J. D'Amico, T. W. Bochow, M. Hmelar, G. R. Marcellino, N. T. Stangos, "Experimental ocular surgery with a high-repetition-rate erbium:YAG laser," *Invest. Ophthalmol. Vis. Sci.*, vol. 39, pp. 1667-1675, 1998.
10. C. C. Neubaur, G. Stevens Jr, "Erbium:YAG laser cataract removal: role of fiber-optic delivery system," *J. Cataract Refract. Surg.*, vol. 25(4), pp. 514-520, 1999.
11. T. Wesendahl, P. Janknecht, B. Ott, M. Frenz, "Erbium:YAG laser ablation of retinal tissue under perfluorodecaline: determination of laser-tissue interaction in pig eyes," *Invest. Ophthalmol. Vis. Sci.*, vol. 41, pp. 505-512, 2000.
12. J. A. Harrington, "A review of infrared fibers," http://irfibers.rutgers.edu/ir-rev-index.html. Adapted from the OSA Handbook, Vol. III, McGraw-Hill. Editor, Michael Bass, 2000.
13. G. N. Merberg, "Current status of infrared fiber optics for medical laser power delivery," *Lasers Surg. Med.*, vol. 13, pp. 572-576, 1993.
14. N. M. Fried, "Potential applications of the Erbium:YAG laser in endourology," *J. Endurol.*, vol. 15(9), pp. 889-894, 2001.
15. M. Mrochen, P. Riedel, C. Donitsky, T. Seiler, "Erbium:yttrium-aluminum-garnet laser induced vapor bubbles as a function of the quartz fiber tip geometry," *J. Biomed. Opt.*, vol. 6(3), pp. 344-350, 2001.
16. N. M. Fried, Z. Tesfaye, A. M. Ong, K. H. Rha, P. Hejazi, "Optimization of the Erbium:YAG laser for precise incision of ureteral & urethral tissues: in vitro & in vivo results," *Lasers Surg. Med.*, vol. 33, pp. 108-144, 2003.
17. Personal communication with Alex Tchap, Infrared Fiber Systems, inc., Silver Spring, MD.
18. N. M. Fried, G. M. Long, "Erbium:YAG laser ablation of urethral and ureteral tissues," *Proc. S.P.I.E.: Lasers Urol.*, vol. 4609, pp. 122-127, 2002.
19. J. M. H. Teichman, K. F. Chan, P. P. Cecconi, N. S. Corbin, A. D. Kamerer, R. D. Glickman, A. J. Welch, "Er:YAG versus Ho:YAG lithotripsy," *J. Urol.*, vol. 165, pp. 876-879, 2001.
20. H. Lee, T. R. Ryan, A. Lee, J. H. Teichman, A. J. Welch, "Feasibility study of Er:YAG lithotripsy," *Lasers Surg. Med.*, Suppl 15:12, 2003.
21. K. F. Chan, H. Lee, J. M. H. Teichman, A. Kamerer, H. S. McGuff, G. Vargas, A. J. Welch, "Erbium:YAG laser lithotripsy mechanism," *J. Urol.*, vol. 168, pp. 436-441, 2002.
22. E. Papagiakoumou, D. N. Papadopoulos, N. Anastasopoulou, A. A. Serafetinides, "Comparative evaluation of HP oxide glass fibers for Q-switched and free-running Er:YAG laser beam propagation," *Opt. Comm.*, vol. 220, vol. 151-160, 2003.

Journal of Endourology
Vol. 17(9), 2003

was measured by energy detector with the laser set at 500 mJ pulse energy at 10 Hz. Pyroelectric imaging was done. The fibers were run at 500–2800 mJ pulse energy to determine the minimum energy required to fracture the fiber at the site of bending. Each fiber was placed through the working channel on the ACMI DUR-8 Elite ureteroscope and flow rates (mL/min) were calculated. The maximum deflection of the DUR-8 Elite with each fiber in the working channel was recorded.

RESULTS: All small fibers had greater optical output in straight vs. 180° configurations. The Dornier fiber had the lowest optical output in either configuration. Some medium fibers had greater optical output in straight vs. 180° configurations. The Dornier 200 μm fiber fractured repeatedly in 180° configuration with pulse energy as low as 0.6 J. The Lumenis 365 μm fiber fractured repeatedly in 180° configuration with pulse energy as low as 1.0 J. Pyroelectric images confirmed near Gaussian optical output for all fibers. Flow rates (mL/min) were calculated with each fiber inserted into the DUR-8 Elite working channel.

	500 mJ pulse energy (50 pulses, 3 runs) Fiber Straight	500 mJ pulse energy (50 pulses, 3 runs) Fiber 180°	Minimum pulse energy (mJ) required to fracture fiber Fiber 180°	Fiber Diameter in microns	Mean flow rate through DUR-8 Elite Ureteroscope (mL/min)	Maximum angle of deflection achieved with fiber with DUR-8 Elite Ureteroscope (°)
Lumenis 272	476 ± 1	408 ± 0	*	407.5	27.7	242
InnovaQuartz 200	408 ± 0	402 ± 1	2800	384	30.0	272
Dornier 200	250 ± 2	243 ± 1	600	354.5	34.2	263
Optical Integ 300	485 ± 1	485 ± 1	*	693	8.8	210
Lumenis 365	501 ± 0	503 ± 0	2000	520	17.2	205
InnovaQuartz 400	498 ± 2	496 ± 0	*	718.5	7.7	210
Dornier 400	506 ± 1	448 ± 1	*	716.5	8.0	206.5

* did not fracture with pulse energy setting up to 2.8J

CONCLUSIONS: Optical performance differs among manufacturers. For small fibers, the Lumenis 272 μm and Innova 200 μm fibers are best. For medium fibers, the Innova 400 μm and Optical Integrity 300 μm fibers are best. The Dornier 200 μm fiber does not couple well with the Lumenis laser.

ABSTRACT 26

Laser Therapy in Penile Carcinoma: Point of Technique and Outcome

Dominic Frimberger, Edwin Hungerhuber, Alfons Hofstetter, and Peter Schneede
Department of Urology, Ludwig-Maximilians University of Munich Grosshadern, Munich, Germany

The most important issues in penile cancer remain adequate tumor control and the prevention of recurrent disease. The outcome data from a single institution of the last 13 years for patients with penile carcinoma treated with Nd:YAG laser coagulation was reviewed to evaluate the safety of laser treatment in comparison to local excision and amputation techniques respectively. A retrospective analysis of 29 patients with penile carcinoma treated with Nd:YAG laser coagulation between 1987 and 2000 was performed. Two patient groups were formed, group 1 consisting of patients with carcinoma in situ only and group 2 including all other tumor stages. Group 1 consisted of 17 patients of which 2 had recurrent disease. Two patients underwent inguinal lymphadenectomy of which one was positive. Group 2 consisted of 12 patients, 10 with T1 disease and 2 with a T2 tumor. One patient developed recurrent disease and 2 patients had metastatic spread to their lymph nodes. Two patients, one of each group required partial amputation for recurrent disease. The cosmetic results and patient satisfaction are excellent. Modern laser surgery of the outer genital allows oncologically, functionally and cosmetically convincing results in the hand of the experienced surgeon. While superficial lesions up to T1 can safely be treated with Nd: YAG laser coagulation, the treatment of choice for stage T2 or higher lesions remains partial amputation.

ABSTRACT 27

Erbium:YAG Laser Incision of the Ureter and Urethra: Optimization of the Laser Parameters

Nathaniel M. Fried,[1] Albert M. Ong,[1] Koon H. Rha,[1] Zelalem Tesfaye,[1] and Pooya Hejazi[2]
Departments of Urology[1] and Electrical Engineering,[2] Johns Hopkins University, Baltimore, MD

INTRODUCTION: The most frequent complication associated with endourologic treatment of ureteral and urethral strictures is stricture recurrence. The erbium:YAG laser is capable of incision of soft tissues with minimal peripheral thermal damage and therefore may be a promising alternative to the cold knife and Holmium:YAG laser for incision of ureteral and urethral strictures.

METHODS: Optimization of the Er:YAG laser was conducted using fresh samples of porcine ureters and canine urethras, ex vivo. Preliminary in vivo studies were also performed in a laparoscopic porcine ureteral model with exposed ureter. Laser radiation with a wavelength of 2.94 μm, pulse lengths of 8, 70, and 220 μs, output energies of 2–35 mJ, fluences of 1–25 J/cm^2, and pulse repetition rates of 5–30 Hz, was delivered through 250-μm and 425-μm core germanium oxide optical fibers in direct contact with ureteral tissue.

RESULTS: Ex vivo perforation thresholds measured 2–4 J/cm^2, with ablation rates of 50 μm/pulse at fluences of 6–11 J/cm^2. In vivo perforation thresholds were approximately 1.8 J/cm^2, with the ureter perforated in less than 20 pulses at fluences greater than 3.6 J/cm^2. Thermal damage zones ranged from a minimum of 20 μm at 8 μs laser pulse lengths to a maximum of 60 μm with 220μs pulses. Mechanical damage (tissue tearing) was observed with the Er:YAG laser at the 8 μs pulse duration, and operation was limited to low pulse repetition rates.

CONCLUSION: The Er:YAG laser, operating at a pulse duration of approximately 70 □s, a fluence of 4 J/cm^2, and a pulse repetition rate of 20 Hz, is capable of rapidly incising urethral and ureteral tissues, in vivo, with minimal thermal and mechanical side-effects. The Er:YAG laser is more efficient that the Ho:YAG laser for cutting tissue, with perforation thresholds measuring ~2 J/cm^2 versus ~34 J/cm^2, respectively. The Er:YAG laser is also more precise than the Ho:YAG laser, with peripheral thermal damage zones measuring 10–20 μm versus 300 μm, respectively. Chronic animal wound healing studies are planned to quantify scarring induced during Er:YAG laser incision, and optimization of fiber optic delivery systems for endoscopic delivery of mid-infrared laser energy has begun.

ABSTRACT 28

Micro-Inkjet Device for Rapid, Precise, and Noncontact Surgical Marking of Tissues

Rahayu Ramli[1] and Nathaniel M. Fried[2]
Departments of Biomedical Engineering[1] and Urology,[2] Johns Hopkins University, Baltimore, MD

INTRODUCTION: There is a need for improved methods of tissue marking as the applications for laparoscopic surgery increase. The use of a micro-inkjet system for noncontact, rapid, and precise marking of surgical margins prior to excision or morcellation of tissue may provide improved correlation with histologic analysis. The purpose of this study was to optimize the micro-inkjet parameters for noncontact marking of tissue and compare its performance with a syringe-pump used for contact marking of tissue.

METHODS: India ink was used as a sample permanent dye for marking of poster board, kidney, and ureter, during the optimization of micro-inkjet and syringe pump systems. Noncontact dye delivery was studied using a micro-inkjet head (4-mm-diameter × 20-mm-length)

tings of 100, 200 and 300 kPa. Stone phantoms underwent 30 shocks at each respective setting.

Results At 120 mJ the FREDDY laser caused stone retropulsion a mean distance of 3.4, 1.4 and 1.7 cm at settings of 1, 3 and 5 Hz respectively. At 160 mJ the FREDDY laser retropulsed the stone a mean distance of 4.6, 3.7 and 3.5 cm at settings of 1, 3 and 5 Hz respectively. The lithoclast retropulsed the stone a mean distance of 6.1, 9.9 and 11.5 cm at pressure settings of 100, 200 and 300 kPa respectively.

Conclusions Stones were retropulsed a greater distance at lower frequency settings with the FREDDY laser. However, the retropulsion was significantly less than that caused by the pneumatic lithotripter at all settings.

MP06.05

HYBRID GERMANIUM / SILICA OPTICAL FIBERS FOR FLEXIBLE ENDOSCOPIC DELIVERY OF HIGH-POWER ERBIUM:YAG LASER RADIATION

N.M. Fried, C.A. Chaney

Department of Urology, Johns Hopkins Medical School, Baltimore, MD, USA

Introduction The Erbium:YAG laser is more efficient than the Holmium:YAG laser for laser lithotripsy and produces less peripheral thermal damage during laser incision of soft urological tissues. The main factor limiting endourologic use of the Er:YAG laser is the lack of a suitable optical fiber delivery system which is robust, flexible, and biocompatible.

Objective To construct and test an optical fiber capable of transmitting high-power Er:YAG laser radiation through a flexible endoscope for potential use in multiple endourologic procedures, including laser lithotripsy and incision of ureteral and urethral strictures.

Methods Hybrid optical fibers were assembled from 550-mm-core, low-OH silica fiber tips attached to 425-mm-core germanium oxide trunk fibers using four techniques: UV-cured epoxy, steel hypodermic tubing, glass capillary tubing, and heat-shrink tubing. Fiber output energy from the Er:YAG laser (λ = 2.94 mm) was measured during laser operation at a pulse length of 220 ms, pulse repetition rate of 3 Hz, and output energies up to 300 mJ. Preliminary optical fiber bending tests were also performed through a flexible endoscope.

Results The damage threshold for the germanium oxide fibers during contact soft tissue ablation was 9 mJ. For the hybrid germanium / silica fibers, maximum fiber output energies measured 180 ± 30 mJ (n=9) before fiber damage was observed at the fiber interface. This value was above the minimum energy needed for Er:YAG laser ablation of soft ureteral and urethral tissues (~ 8 mJ) and stones (~ 25 mJ).

Conclusion Simple assembly of a hybrid germanium / silica optical fiber may represent a robust, flexible, and biocompatible method of delivering high-power Er:YAG laser radiation during endoscopic procedures.

MP06.06

EFFECT OF INTRANASAL DESMOPRESSIN SPRAY IN THE TREATMENT OF RENAL COLIC

F. Tadayyon, M.R. Ebadzadeh

Department of Urology, Noor Hospital, Esfahan, Iran

Objective To assess the efficacy of desmopressin nasal spray and compared it with diclofenac given intramusculary in patient with acute renal colic.

Methods From March 2001 to October 2002 , 90 patient with acute renal colic, randomized in to three different groups: group A received desmopressin nasal spray (40 microgram), group B received diclofenac intramusculary (75 mg) and group C received both desmopressin (40 microgram) and diclofenac (75 mg). Pain was assessed using a visual analogue scale (a 10 cm horizontal scale ranging from no pain to unbearable pain) at baseline, and at 10 minutes, 20 minutes, 30minutes after administering treatments.

Results In our study 56.6 % of patientes in group A, 86.6 % of patientes in group B, and 90 % of patientes in group C showed either complete relief or relative pain improvment respectively. In this study three type of treatment was effective.(P value less than 0.05) At 10 min the pain decreased in all three groups.There was no significant difference between group A and group B and also between groupB and group C, but significant difference is noted between group A and C.(P value less than 0.05). At 20 and 30 min there was significant difference between group A and B and also between group A and C(P value less than 0.05),but no difference between group B and C.

Conclusion Desmopressin has several advantages, e.g. ease of administration and lack of important side effects which make it suitable for ambulatory use. Desmopressin acts rapidly and seems to be effective in both single and combined therapy with diclofenac and increases the analgesic effect of diclofenac.

MP06.07

THE EFFICACY OF PAPAVERINE HYDROCHLORIDE FOR PAIN RELIEF IN PATIENTS WITH RENAL COLIC AS A SINGLE AGENT AND IN COMBINATION WITH SODIUM DICLOFENAC (NSAIDS)

N. Snir, B. Moskovitz[1], O. Nativ[1], P. Livne, D. Lifshitz

Department of Urology, Rabin Medical Center, Petah-Tiqwa; Department of Urology, Bnai-Zion Medical Center[1], Haifa; Israel

Acute renal colic is one of the most anguishing forms of pain that needs quick and effective pain relief treatment. Three drug groups are commonly used: NSAIDS, Opioids and smooth muscle relaxants. The analgesic effect of NSAIDS and Opioids has been widely researched while the role of smooth muscle relaxants is less clear in the treatment of renal colic.

Objective To assess the efficacy of Papaverine Hydrochloride - a commonly used muscle relaxant, as a single agent and in combination with Sodium Diclofenac, in the treatment of renal colic.

Methods In a single blind, randomized, multi-center clinical trial, 86 patients were admitted to the E.R for renal colic. Treated either with 120 mg of I.V Papaverine Hydrochloride (29 patients-group 1), 75 mg I.M Sodium Diclofenac (30 patients-group 2) or the combination of both (27 patients-group 3). Evaluations by V.A.S (Visual Analogue Scale 0 to 10) was assessed at 0, 20 and 40 minutes after treatment .If insufficient analgesia was achieved, 1 mg/kg of Pethidine (I.M) was admitted